An Algorithmic Information Calculus for Causal Discovery and Reprogramming Systems

Hector Zenil^*[a,b,c,d,e], Narsis A. Kiani*[a,b,c,d,e], Francesco Marabita[b,d], Yue Deng[b], Szabolcs Elias[b,d], Angelika Schmidt[b,d], Gordon Ball[b,d], & Jesper Tegnér^[b,d,f]

a) Algorithmic Dynamics Lab, Center for Molecular Medicine, Karolinska Institutet, Stockholm, 171 76, Sweden
b) Unit of Computational Medicine, Center for Molecular Medicine, Department of Medicine, Solna, Karolinska Institutet, Stockholm, 171 76, Sweden
c) Department of Computer Science, University of Oxford, Oxford, OX1 3QD, UK.
d) Science for Life Laboratory, Solna, 171 65, Sweden
e) Algorithmic Nature Group, LABORES for the Natural and Digital Sciences, Paris, 75006, France.
f) Biological and Environmental Sciences and Engineering Division, Computer, Electrical and Mathematical Sciences and Engineering Division, King Abdullah University of Science and Technology (KAUST), Thuwal 23955–6900, Kingdom of Saudi Arabia

* Shared-first authors
^ Corresponding authors

Author Contributions: HZ, NK and JT are responsible for the general design and conception. HZ and NK are responsible for data acquisition. HZ, NK, YD, FM, SE and AS contributed to data analysis. HZ developed the methodology with key contributions from NK and JT. HZ undertook most of the numerical experiments with YD and FM contributing. HZ, GB and SE contributed the literature-based Th17 enrichment analysis. HZ and JT wrote the article with key contributions from NK. Correspondence should be addressed to HZ: hector.zenil@algorithmicnaturelab.org and JT jesper.tegner@kaust.edu.sa

The Online Algorithmic Complexity Calculator implements the perturbation analysis method introduced in this paper: http://complexitycalculator.com/ and an online animated video explains some of the basic concepts and motivations for general understanding: https://youtu.be/ufzq2p5tVLI

Abstract:

We introduce a conceptual framework and an interventional calculus to steer, manipulate, reconstruct the dynamics and generating mechanisms of dynamical systems from partial and disordered observations based on the contribution of each of the system's by exploiting first principles from the theory of computability and algorithmic information. This calculus consists in finding and applying controlled interventions to an evolving object to estimate how its algorithmic information content is affected in terms of *positive* or *negative* shifts towards and away from randomness in connection to causation. The approach is an alternative to statistical approaches to infer causal relationships and to provide theoretical expectations from perturbation analysis. We find that the algorithmic information landscape of a system's runs in parallel to its dynamic landscape providing a path to move systems on one plane to have controlled effects on the other plane. Based on these methods, we advance tools for reprogramming a system that do not require full knowledge or access to the system's actual kinetic equations or to probability distributions. This new dimension provides a suite of powerful parameter-free algorithms of wide applicability ranging from causal discovery, dimension reduction, feature selection, model generation, a maximal algorithmic-randomness principle and a system's (re)programmability index. We apply these methods to static (e.coli Transcription Factor network) and to evolving genetic regulatory networks (differentiating naïve to Th17 cell, and the CellNet database). We show the capabilities to pinpoint key elements (genes) related to cell function and cell development conforming with the biological knowledge from experimentally validated data and the literature demonstrating how the method can reshape a system's dynamics in a controlled manner through algorithmic causal mechanisms.

Introduction

How to make optimal predictions about the behaviour of dynamical systems is a fundamental problem in science. It remains a challenge how to understand and ultimately reprogram the behaviour of such systems with access to partial knowledge and incomplete or noisy data. Based on established knowledge drawn from the mathematical theories of computability and algorithmic probability that describe the limits of optimal characterization and algorithmic inference, we introduce a conceptual framework with specific methods and applications to demonstrate the use and advantage of a powerful calculus based on the change of a system's algorithmic content over time and under perturbations.

At the core of the causal calculus is the estimation of the specific sequence of events—in the form of perturbations—that rank a system's elements by the effects they can exert on the whole system towards manipulating its fate and function. We will demonstrate that manipulating and reprogramming systems on the algorithmic-information space runs in parallel to the dynamic state/attractor space on which a network or a system can be moved through optimized paths in different directions. Based on universal principles of the most powerful theory of induction and inference (namely algorithmic probability) and recent numerical advances to produce estimations we introduce a suite of powerful parameter-free algorithms to tackle the challenge of causal discovery of generating mechanisms to effectively and efficiently control the dynamics of general systems without knowing kinetic equations for expensive simulations, artificially assuming non-linearity or underlying probability distributions.

The main idea behind the algorithmic causal calculus is based upon evaluating the algorithmic information of dynamical objects, such as strings or networks changing over time. Let S be a non-random binary file containing a string in binary:

10101010101010101010101010101010101010101010101010101010101010101010101010

Clearly, S is algorithmic compressible with p_S ="Print(01) 35 times" a short computer program generating S. Let S' be equal to S except for a bitwise operation (bitwise NOT, or complement) in, say, at position 24:

10101010101010101010100101010101010101010101010101010101010101010101010101

A short computer program that generates S' can be written in terms of p_S that can already account for most of the string except for the perturbed bit which $p_{S'}$ has thus to account for. A candidate program can be $p_{S'}$ ="Print(10) 11 times; Print(00); Print(10) 23 times". Clearly, the length in binary of the computer program p_S generating S is upper bounded by $|p_{S'}|$, the length, in bits, of the computer program $p_{S'}$ generating S'. Otherwise said, assuming shortest computer programs, we have $C(S) < C(S')$ for any single-bit mutation of this string S, where $C(S) = |p_S|$ and $C(S') = |p_{S'}|$ the lengths of the shortest computer programs generating S and S'.

Without loss of generalization, let now S be a binary file of the same size but consisting of, say, random data:

01101100100011001101010001110110001100011010011100010000110011001100011

where S is now algorithmically incompressible. This means that S has no generating mechanism shorter than the string itself and can only be generated by a computer program of the form p_S = Print(S), which is not much shorter than S itself. Let S' be the result of negating any bit in S just as we did for S and S', then $p_{S'}$ = Print(S'). Then there are 2 possible relations between $p_{S'}$ and p_S after a single bit perturbation (bit negation), either $p_S < p_{S'}$ or $p_S > p_{S'}$ depending on S' moving towards or away with respect to C(S). However, perturbing only a single bit cannot result in a (much) less random S' because p_S = Bitwise(Print(S'),n) can be used to reverse S' into S which is random, but both Bitwise and n (the bit index to be changed) are of fixed and small length and so do not contribute to the already high algorithmic complexity/randomness of the original random string (which can be of any length) hence in contradiction with the original assumption that S is algorithmic random (or not compressible).

This means that perturbations to an algorithmically random object have lower impact to their generating mechanism (or lack of) than to non-random objects, with respect to the generating mechanisms of their unperturbed states and thus this effect can be exploited to estimate and infer the causal content of causal or non-causal objects. In an algorithmic random object, any change goes unnoticed because no perturbation can lead to a dramatic change of its (already high) algorithmic content. Interesting cases, far from these simplistic examples, will move in an intermediate region towards both directions, towards and away from randomness, and are also interesting to study as capable of moving in both directions and thus *algorithmically 'reprogrammable'*.

Let {S'} be the set of all possible mutated strings of S, and S'_n an instance in {S'} with n from 1 to the power-set cardinality of |S'| the length of S, then each evaluation of $C(S'_n)$ represents the length of a possible generating mechanism accounting for each perturbation, intervention, past or future evolution of a string as a dynamic object changing from S to S'_n. These models and trajectories have the advantage to highlight the principles by which a system or a network is organized uncovering candidate mechanisms by which it may grow or develop. The causal calculus consists thus in studying the algorithmic-information dynamic properties of objects to construct an algorithmic-information landscape to identify and rank the elements by their algorithmic contribution and the changes they may exert on the original object to move it towards or away from randomness. In what follows, we demonstrate that insights coming from the algorithmic information landscape can effectively be used to find and unveil the dynamics and reprogramming capabilities of the systems, starting from a reconstruction of space-time dynamics and their initial and boundary conditions, helping infer the (most algorithmic likely) generating mechanism of an evolving system from a set of (partial and even disordered) observations (see Fig. 3). We will explore the capabilities of this calculus to characterize genes in regulatory networks and to reprogram systems and networks in general, including specific examples, both theoretically and experimentally on synthetic and biological data.

An Algorithmic Causal Perturbation Analysis for Systems and Networks

In practice, estimating $C(S_t)$ is characterized as *lower semi-computable* meaning that it can only be approximated from above. Recent numerical advances—alternative to lossless compression algorithms—have led to sound estimations[4,5] of *Algorithmic Probability*[2,3] that can go beyond statistical regularities and are better equipped to produce causal models[6] because a truly algorithmic estimation of *algorithmic complexity, denoted by* C(S) implies, by definition,

finding short computer programs accounting for an observation and so the estimation entails finding algorithmic models reproducing strings like S or versions close to S that can be aggregated. The use of such novel methods have already found a wide range of applications in areas such as cognition[7,8]. Here we take advantage of these concepts and numerical advances to tackle the problem of finding mechanisms of design and control of systems.

Algorithmic Probability (AP)[2,3,9] deals with the challenge of inductive inference[10], and it is the obverse of the rigorous mathematical formalization of (algorithmic) randomness[1,3,9,11] by way of the so-called (algorithmic) *Coding theorem*[3] formally described by $C(s) \sim -\log_2 AP(s)$ Supplement Section 1) relating complexity C and probability AP. For example, the AP(G) of a causal graph or network G can be defined[12] as the probability that a random computer program constructed bit by bit–by, e.g., random flips of a coin–outputs a (lossless) description of G, d(G), e.g. its adjacency matrix. Because AP is *upper semi-computable* it allows algorithmic complexity C to be approximated. Among the most remarkable properties of AP and C is that they cannot be refuted at an arbitrary significance level by any computable measure[3], and estimations of C(d(G)) asymptotically converge to C(G), independently of d, up to a relatively small constant[2,9,11] (Supplement Section 1, *invariance theorem*). The idea behind the numerical methods to estimate AP[4,5] is to enumerate the set of computer programs that explain and generate in full or part the generating system representing the predictive computational model of the observables (Supplement Section 1, *CTM* and *BDM* methods).

In a deterministic dynamic system s, the length of the shortest generating mechanism f describing a system's state (in binary) at time t, denoted by $C(s_t)$, can only grow by a function of t, more specifically $\log_2(t)$. This is because in a deterministic dynamic system, every state s_{t+1} can be calculated from s_t from $s_{t+1} = f(s,t)$. This trivial but fundamental property of deterministic dynamic systems can be exploited to find the set of perturbations on a system's state s_t related to a set of perturbations $s_{t'}$ such that deviations from $\log_2(t)$ indicate non-causal trajectories and disconnected patches unrelated to the original dynamic system upon performing observations. When a system is not completely isolated and some of its parts seem to be not explained by any other state of the system thereby appearing non-deterministic, those patches can be exposed and identified as foreign to the system's normal cause in the algorithmic perturbation analysis.

We estimate the change of algorithmic information in a network G after an intervention. We define an element e to be *negative* if $C(G) - C(G\backslash e) < 0$, where $G\backslash e$ is a mutated network G without element e, moving G towards algorithmic randomness, *positive* if $C(G) - C(G\backslash e) > 0$, and *neutral* otherwise (Fig. 1a-e). A *maximally random network* (Fig. 1c) has only *positive* (blue) elements because there exists no perturbation that can increase the randomness of the network either by removing a node or an edge, as it is already random (and thus non-causal). We denote by *spectra*(G) the list of non-integer values quantifying the information-content contribution of every element (or subset of elements) of G (Fig. 1f), while σ(G), denotes the *signature* of G, the sorted version from largest to smallest value in spectra(G). This simple set is informative enough to allow an ab-initio identification of the vulnerable breaking points in regular S-W networks (Fig. 1k), whereas the removal of neutral elements (Fig. 1l) minimizes the loss of information relevant to the description of a network, if important, such as graph theoretic properties (Fig. 1l) and its *graph spectra* (by design), as it preserves the overall algorithmic information content and thus establishes a powerful optimal parameter-free method for dimensionality reduction (Supplement Section 2 & Methods). To save computational resources, in numerical experiments we will mostly consider single perturbations only rather than the full power-set of them.

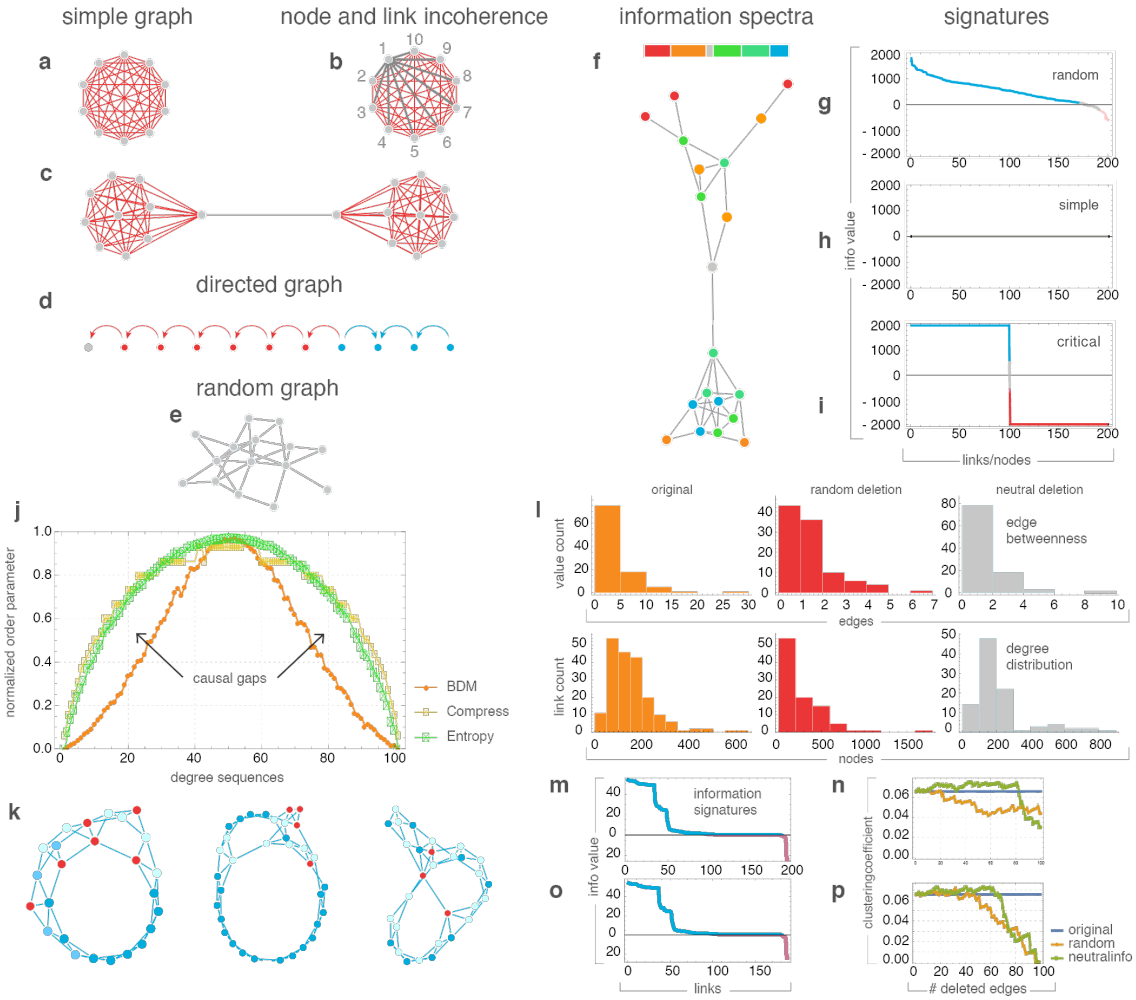

Fig 1. Networks as Computer Programs: **(a)** Nodes and edges identified according to their information contribution to each network by evaluating the effect they have upon removal, red: the element moves the network towards randomness, gray: moves the network away from randomness by a logarithmic factor only, hence neutral. **(b)** *Neutral information set*: removal of node 1 is equivalent to the removal of all the edges connecting to node 1, even though all the individual edges are negative by themselves (we call this effect 'incoherence'). **(c)** All nodes and edges in a non-recursive random graph are neutral because no element can (significantly) move the network towards randomness (or simplicity). **(d)** A random connection between two complete graphs is positive because its removal makes the generating mechanism of 2 complete graphs shorter than the 2 complete graphs randomly connected. **(e)** Information analysis on a directed graph identifies changes of direction. **(f)** The *information spectrum* identifies the different contribution and capabilities of all elements in a spectrum. **(g,h,i)** The *signature* of a graph is the *info spectrum* sorted from highest to lowest information content. **(j)** Causal discovery gain using algorithmic information vs methods such as Entropy and compression over a set of fixed length strings normalized by maximum Entropy, some strings are less random than Entropy and lossless compression suggest. **(k)** Inverse spectrum colouring identifies breaking points in randomly rewired regular graphs. **(l)** Neutral node and neutral edge removal preserves *signature* and other properties such as edge betweenness **(i top),** degree distribution **(l bottom)** and clustering coefficient **(n,p)** thus optimal for dimensionality reduction (see MILS SI).

Since neutral elements do not contribute to the algorithmic content of a system they do not affect the length of the underlying generating program, which means that the network can recover those neutral elements at any moment by simply running the system back to the point when the elements were removed (Fig. 2a). This process of identification of algorithmic contributing elements allows systems to be 'peeled back' to their most likely causal origin, unveiling their generating principles (Supplement Section 2), which can then be used as a handle to causally steer a system (Fig. 2b,c) where other measures fail (Fig. 2d, Extended Data Fig. 2) [6]. Analogously, elements can be added to a network to increase or maximize its algorithmic information content, thus approximating a *Maximally Algorithmic-Random (MAR) graph* that can be used for maximum-entropy modelling purposes, with the advantage of discarding false maximal entropy instances (Supplement Section 2). In contrast to neutral elements, extreme (negative or positive) valued network elements hold and drive the network towards or away from algorithmic randomness. This extends our view of the nature of a network (Extended Data Fig. 1).

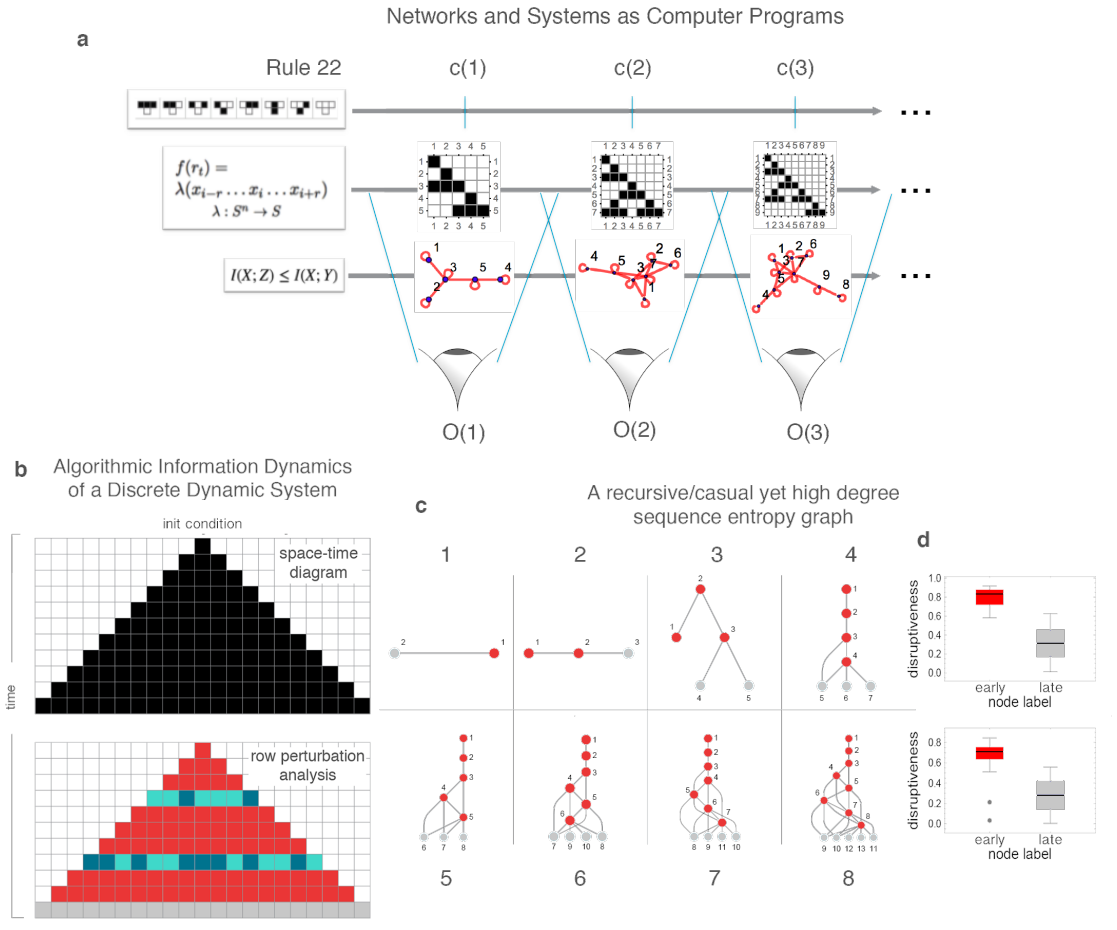

Figure 2. (a) The introduced causal calculus can help reveal the generating mechanisms of any system disregarding the different representations that a dynamical system may have both in their origin or their effects, yet the methods introduced aim at the most algorithmic (causal) version if there is one (non-random objects). **(b)** A one-dimensional evolving system displays the

same information elements determining the different causal regions after an instantaneous observation following a perturbation analysis. In a Cellular Automata, after 2 random row perturbations a new information analysis reveal which are the rows that have been artificially perturbed, with grey cells showing the identified neutral row, the last (top-down) in the dynamic evolution, indicating the time direction of the system. See Fig. 3 **(c)** Unlike (a), Entropy is not invariant to different object descriptions. Shown here is a tree-like representation of a constructed causal network with low algorithmic randomness but near maximum Entropy degree sequence (SI 8), a contradiction, given the recursive nature of the graph and the zero Shannon entropy rate of its adjacency matrix diverging from its expected Shannon entropy. **(d)** Latest nodes in the same graph depicted in (c) are identified by their neutral nature, revealing the time order and thereby exposing the generating mechanism of the recursive network (for details see SI 8, and SI 4).

In Fig. 3 we demonstrate how the algorithmic calculus can help reconstruct discrete dynamic systems (illustrated using 1-dimensional cellular automata called Elementary Cellular Automata or ECA) with high accuracy from disordered states and even index observations correctly effectively providing a mechanistic generating model that can be run backward and forward in time. This is because late perturbations are more akin to a neutral information value (as established, in deterministic systems they should contribute at most log n, with n representing the step index of the dynamical). That we can reconstruct the space-time evolutions and rules from the disordered output of an abstract computing model (cellular automata) by using an empirical distribution constructed from a different model of computation (Turing machines) is an indication of the robustness of both theory and methods.

That we can reconstruct the space-time evolution of discrete dynamical systems with high accuracy from an instantaneous non-ordered set of observations (rows) demonstrates that we identify them as causal even among those random-looking such as ECA rules 73, 45 and 30 for which correlation values rho (Fig. 3) may be lower but reconstructions are still qualitatively close. By using the results that the latest steps in time in a dynamical system such as an elementary cellular automata the less disruptive the effect of the perturbation respect to the algorithmic-information of the original system, we were able not only to reconstruct the cellular automata after row-scrambling but we gave each row a time index (Fig 3b). The automatic reconstruction of possible generating mechanisms by quantifying how disruptive is a perturbation in the algorithmic information content of the space-time evolution of a CA, we can extract the generating mechanism from the order in which perturbations are less to more disruptive in the hypothesized generating mechanism inferred from an instantaneous observation. Apparent simpler rules have simpler hypotheses with an almost perfect correspondence in row order (Fig. 3a,b second columns from each pair). Some systems may look more disordered than others but locally the relationship between single rows is mostly preserved even among the more random-looking, either in the right or exact reverse order (indicating possible local reversibility).

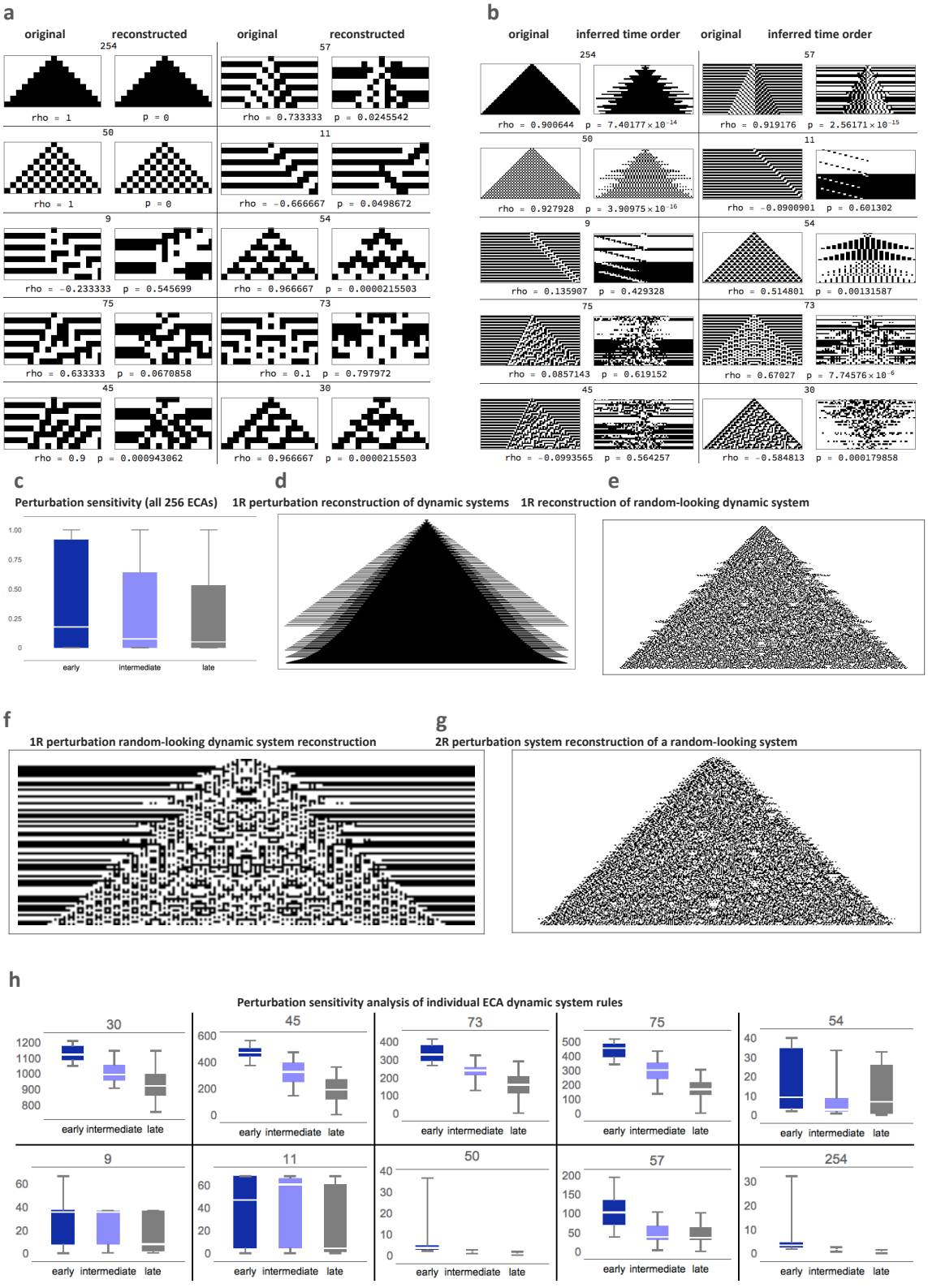

Figure 3. (a) Reconstruction of the space-time evolution of dynamic systems (Elementary Cellular Automata or ECA[19]). Normal space-time evolution is displayed on the left-hand-side, on the right-hand-side are the reconstructed space-time after row scrambling by finding the lowest

algorithmic complexity configuration among all possible 9! = 362880 row permutations (8 steps + initial configuration). All followed by Spearman correlation values for row order. **(b)** Row time inference in linear time by generation of an algorithmic model that can run forward and backward thus revealing the dynamics and first principles of the underlying dynamic systems without any brute force exploration or simulation. **(c)** As predicted, the later in time a perturbation is performed the less disruptive (change of hypothesized generating mechanism length after perturbation) compared to the length of the hypothesized generating mechanism of evolution of the original system. Each pair shows the statistic rho and p values between the reconstructed and original space-time evolutions. With some models separating the system into different apparent causal elements. **(d)** Depicted is the reconstruction of one of the simplest elementary cellular automata (rule 254) and **(e)** one of the most random-looking ECAs both after 280 steps illustrating the perturbation-based algorithmic calculus for model generation in 2 opposite behavioural cases. **(f)** and **(g):** The accuracy of the reconstruction can be scaled and improved at the cost of greater computational resources by going beyond single row perturbation up to the power-set (all subsets), here depicted are reconstructions of random-looking cellular automata (30 and 73 running for 200 steps) from single (1R) and double-row-knockout (2R) perturbation analysis. Errors inherited from the decomposition method (see SI, BDM) look like 'shadows' and are explained (and can be counteracted) by numerical deviations from the boundary conditions in the estimation of BDM[20]. **(h)** Variations of the magnitude of the found effect is different in systems with different qualitative behaviour, the simpler the less different the effects of deleterious perturbations at different times.

Algorithmic Information Connection to Dynamical Properties

Since our calculus can trace the generative structure in an algorithmic sense, we have shown that we can distinguish causal systems from non-causal systems (Fig. 1j). From a mathematical standpoint we have it that for every non-random network, there exists a generative (causal) program of a certain size (represented, e.g., by its degree sequence or any lossless matrix representation). In contrast, if a network has no shorter (lossless) description than itself, then it has no generative causal program and is defined as *algorithmic random*. This very generative program and the number of possible halting states, which it can be driven into, determine the number of attractors in a dynamical system. In a network with internal dynamics, both topological and kinetic details can be encoded in a full lossless description, and can thus be handled by the algorithmic causal calculus introduced here. Observations over time are the result of these two factors, but with no access to the generative program, deconvolution of all the measured elements contributing to the underlying system's dynamics is impossible, and we usually only keep a partial account of the system's dynamic output (see Fig. 2a; Supplement Section 2).

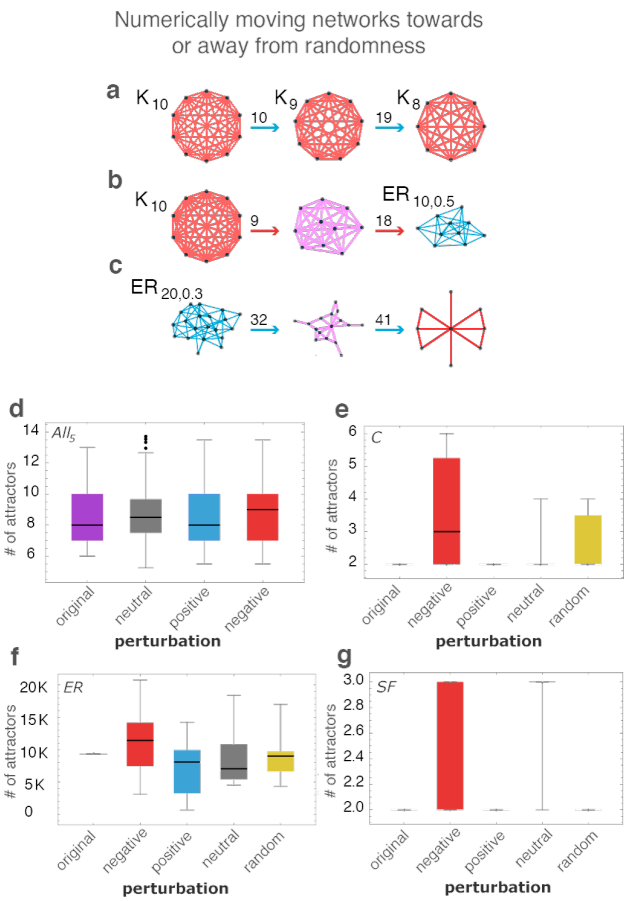

Figure 4. **(a)** Numerically pushing a complete graph away from randomness by edge deletion produces complete graphs (after 10 and 19 steps from step 1) as theoretically expected. **(b)** Pushing a network towards randomness produces ER graphs approaching edge density (d = 0.5). **(c)** Pushing a random graph towards simplicity reveals (after 32 and 41 steps) structured subgraphs nested in the original random one. **(d)** Distributions (SI 6) of the number of attractors for all possible 5-node Boolean networks. The small difference is significant because the number of attractors in such small graphs is tightly bounded. **(e)** Numerical calculation of the change in number of attractors in simple directed complete graphs, ER and scale-free networks converted into Boolean networks (SI 5 and 6). Scale-free networks, like regular networks, are more resilient in the face of perturbations.

This algorithmic calculus enables the identification of a system's causal core and facilitates the assessment of the causal contribution of a system's elements (detailed in Supplement Section 1 and 2). We evaluated whether this calculus could serve as a guide to reprogramming a system represented by a network corresponding to qualitative shifts in the *attractor landscape* associated with the system's behaviour, even in the absence of access to the dynamical system' s equations. In low algorithmic content networks such as a complete graphs, all nodes are immune to perturbations up to a logarithmic effect, leaving the basins of attraction and number of attractors the same (as a function of graph size only). *MAR graphs* (Supplement Section 2), however, have no (algorithmic or statistical) structure (by definition), and are thus predicted to have numerous shallow attractors. Moving an ER MAR network away from randomness will thus have an effect on the number and depth of its attractors, as it moves all the way away from randomness. Conversely, networks removed from randomness (e.g. a

simple directed regular graph) have fewer but deeper attractors, but moving them towards randomness will eventually increase the number of attractors and decrease their average depth. These theoretical inferences are confirmed through simulation of Boolean networks (see Fig. 4d-g; Supplement Section 2). Based upon these principles, using, e.g., complete graphs as a model, we could predictively push networks towards and away from randomness (Fig. 4a-c). We also emulated Boolean dynamic networks with different topologies, predicting the nature and change in number of attractors (Extended Data Fig. 4 & SI Section 1) after pushing networks towards or away from (algorithmic randomness).

Application to Networks, Reconstruction of Epigenetic Landscapes, and (Re)Programmability

From these first principles, where systems which are far from random, displaying an inherent regular structure, have relatively deeper attractors and are thus more robust in the face of stochastic perturbations, we derived a *(re)programmability index* according to which algorithmic causal perturbations of network elements pushing the system towards or away from algorithmic randomness reveal qualitative changes in the attractor landscape in the absence of a dynamical model of the system. A network is thus more *(re)programmable* if its elements can freely move the network towards and away from randomness. Formally, the *relative programmability* of a system G, $R_r(G)$ is defined by $P_r(G) := MAD(\sigma) / n$ or 0 if n = 0, where n := *max*(|σ|) and MAD is the *median absolute deviation* (Supplement Section 1).

If σN(G) are the elements that move G towards randomness, and σN(G) the elements that move G away from randomness, then the *absolute programmability* $P_A(G)$ of G is defined as $P_A(G) := |S(\sigma P(G)) - S(\sigma N(G))| / m$, where m := max(S(σP(G)), S(σN(G))) and S is an interpolation function. In both cases, the more removed from 0 the more reprogrammable, and the closer to 1 the less reprogrammable. We then take as the *combined reprogrammability* of G the norm of the vector $||V_R(G)||$ on a *programmability space* given by the Cartesian product $P_r(G) \times P_A(G)$ (Supplement Section 1). These indices assign low values to simple and random systems and high values only to systems with non-trivial structures, and thus constitute what are known as measures of sophistication, in this case quantifying the algorithmic plasticity and resilience of a system in the face of causal perturbations (Extended Data Fig. 3).

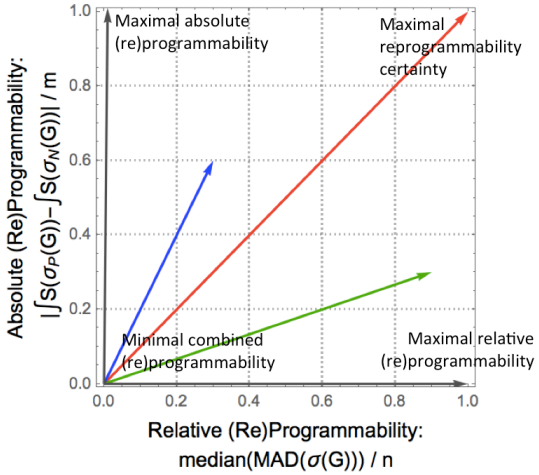

Figure 5. (previously Extended Figure 7.) Illustration of the (re)programmability space defined by the Cartesian product of $(P_r(G) \times P_A(G))$, i.e. the (re)programmability indexes $P_r(G)$ and $P_A(G)$

in a 2-dimensional vector space. *Relative (re)programmability* $P_r(G)$ takes into account the sign of the different segments of σ(G), i.e. how much of a signature segment is below or above zero not immune to small (convergent) numerical errors due to boundary conditions[1], whereas the *absolute (re)programmability* $P_A(G)$ accounts for the shape of the signature σ(G), i.e. how much the signature deviates from e.g. a normal or uniform distribution (Supplement, section1). Both of these indices contribute to the information about the (re)programmability capabilities of a system such as a network. The combined version is, effectively, a weighted index between the two (re)programmability measures that maximizes certainty measured by the magnitude of the vectors, where the closer to (1,1) or (re)programmability vector of magnitude $\sqrt{2}$ the greater the certainty of G to be (re)programmed.

We tested whether this algorithmic causal calculus can provide biological insight and has any explanatory power. First, we applied the calculus to an experimentally validated TF network of E-coli[13] (Fig. 4a). The negatively labelled genes (nodes) protect the network from becoming random and they were therefore found to be the genes that provide specialization to the cellular network, whereas positive nodes (genes) contribute to processes of homeostasis, pinpointing the elements of the network that make it prevail, since their removal would deprive the network of all its algorithmic content and thus of its most important properties. Then we analyzed a network controlling cell differentiation to assess the informative value of the qualitatively reconstructed attractor/differentiation landscape.

Proceeding from an undifferentiated cell state towards a more mature cell state, our calculus predicts fewer but deeper attractors in the differentiated state (Supplement Section 3). In Figure 4b-d, we follow the process from a naive T cell differentiating into a Th17 cell signature[14]. This revealed an *information spectrum* with significantly different values over time and the *(re)programmability* (ratio of negative versus positive edges) was significantly higher in the first two time-points than in the final terminal time-point. Interestingly, the Th17 network signatures suggest information stability at the 48th point where only 3 nodes (STAT6, TCFEB and TRIM24) can further move the network towards greater randomness. After a gene enrichment analysis (Fig. 4b,c,d; Supplement Section 3, Extended Data Fig. 4), genes classified as having the most positive or negative information values comprised many genes known to be involved in T cell differentiation, such as transcription factors from the IRF and STAT families. Finally, retrieving network data from CellNet[15], we reconstructed heights in a corresponding epigenetic Waddington landscape for different cell types conforming to the biological developmental expectation (Fig. 4e; Supplement Section 3).

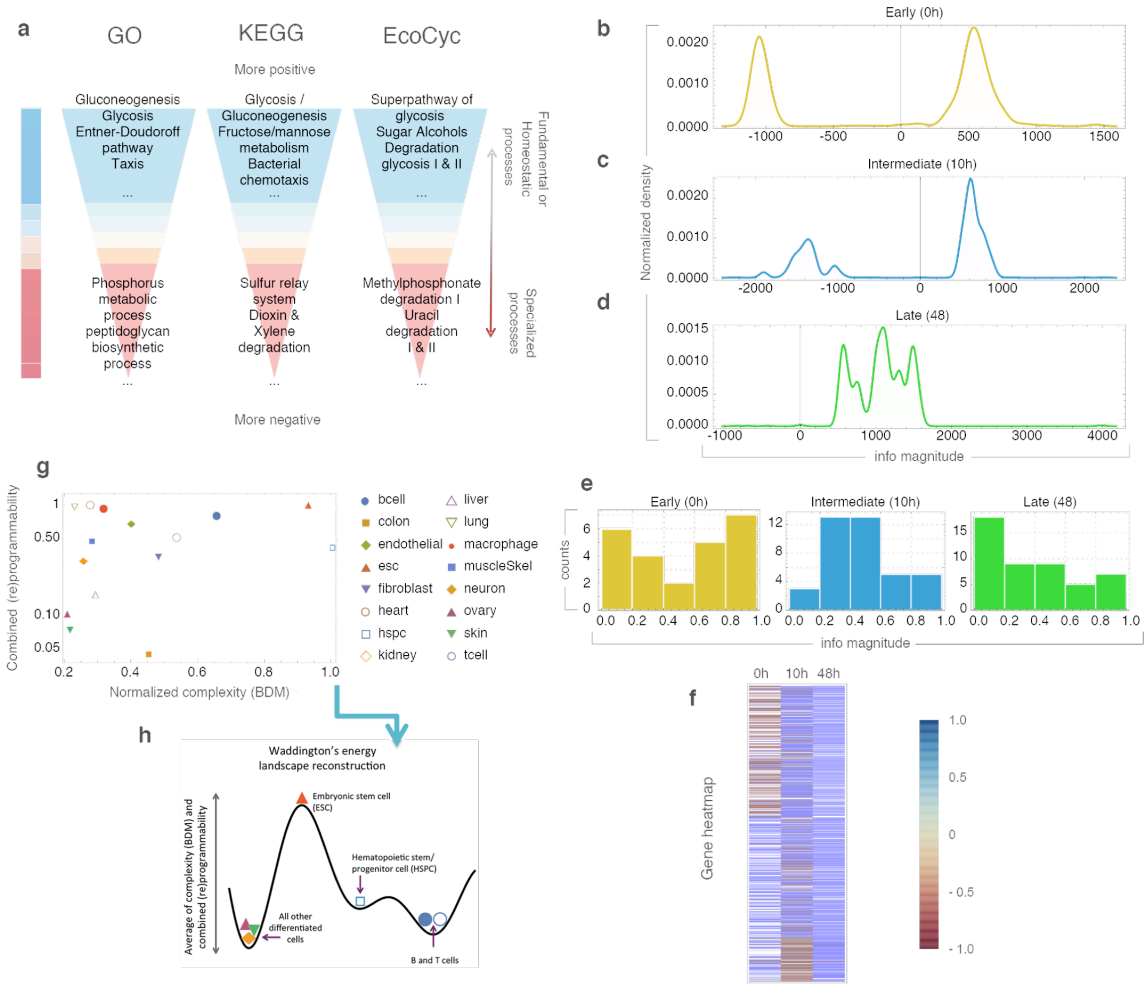

Figure 6. **(a)** K-medoid clustering of transcription factors by algorithmic-information node perturbation analysis on a validated e.coli network (SI 7) according to GO, KEGG and EcoCyc. Positive genes were found to be related to homeostasis while negative genes to processes of specialization. **(b-d)** Distribution of genes according to their causal information value in the differentiation process from CD4+ to Th17 cells. **(e)** Uneven distribution of genes by information value strengthens the significance of the enrichment analysis (see Extended Figure 3). **(f)** Heatmap of normalized information values with approximately half the genes (Early) able to move the early network towards or away from randomness. Genes turn positive at the differentiated stage. **(g)** Charting the regulatory networks (for different cell-types from the Cellnet database using their complexity and *combined programmability*. (h) A sketch of the suggested epigenetic differentiation landscape reconstructed from the average of the reprogrammability and the algorithmic randomness (BDM) (see SI 1) for each cell network.

Conclusion

To summarize, the prevailing paradigm in system identification and control[16,17] can broadly be described as aiming to understand what the relevant features are in a system to formulate models to fit some properties of interest and then maximize the fitting of the model with respect to these properties. An unbiased identification of features is an NP complete

problem, unless additional assumptions are made on the nature of the underlying data-distribution[18]. Thus despite advances in computational tools and fitting data—big or not—to a particular model, the issue of which the relevant properties are upon which to perform the model maximization or error minimization is unresolved. Since the causal calculus here introduced is based on fundamental mathematical results in algorithmic information theory, in combination with novel schemes for numerical evaluations, we have advanced a model-free proxy with which to estimate the qualitative shape of the dynamic possibilities of a system and thus make educated assumptions beyond current statistic approaches. Such an approach gives us a handle to intervene in and steer a system using these powerful parameter-free algorithms. Our results bridge concepts across disciplines and connect mature mathematical theories such as computability, algorithmic complexity and dynamic systems with the challenge of causality in science.

References

1. Martin-Löf, P. The Definition of Random Sequences. *Inf. Control* **9,** 602–619 (1966).
2. Solomonoff, R. J. A Formal Theory of Inductive Inference. Part I. *Inf. Control* **7,** 1–22 (1964).
3. Levin, L. A. Laws of information conservation (nongrowth) and aspects of the foundation of probability theory. 206–210 (1974).
4. Delahaye, J. & Zenil, H. Numerical evaluation of algorithmic complexity for short strings : A glance into the innermost structure of randomness. *Appl. Math. Comput.* **219,** 63–77 (2012).
5. Soler-Toscano, F., Zenil, H., Delahaye, J.-P. & Gauvrit, N. Calculating Kolmogorov complexity from the output frequency distributions of small Turing machines. *PLoS One* **9,** e96223 (2014).
6. Zenil, Hector; Kiani, Narsis;Tegner, J. Low-algorithmic-complexity entropy-deceiving graphs. *Phys. Rev. E - Stat. Nonlinear, Soft Matter Phys.* 96, 012308 (2017).
7. Gauvrit, N., Singmann, H., Soler-Toscano, F. & Zenil, H. Algorithmic complexity for psychology: A user-friendly implementation of the coding theorem method. Behavior Research Methods, Volume 48, Issue 1, pp. 1-16, 201522 (2014).
8. Gauvrit, N., Zenil, H., Soler-toscano, F., Delahaye, J. & Brugger, P. Human behavioral complexity peaks at age 25. *PLoS Comput Biol* **13(4): e10,** (2017).
9. Chaitin, G. J. On the length of programs for computing finite binary sequences. *ACM* **13,** 547–569 (1966).
10. Rathmanner, S. & Hutter, M. A philosophical treatise of universal induction. *Entropy* **13,** 1076–1136 (2011).
11. Kolmogorov, A. N. Three approaches to the quantitative definition of information. *Probl. Peredachi Informatisii* **1,** 3–11 (1965).
12. Zenil, H., Soler-toscano, F. & Dingle, K. Correlation of automorphism group size and topological properties with program-size complexity evaluations of graphs and complex networks. *Physica A* **404,** 341–358 (2014).
13. Marbach, D. *et al.* Wisdom of crowds for robust gene network inference. *Nat Methods* **9,** 796–804 (2012).
14. Yosef, N. *et al.* Dynamic regulatory network controlling TH17 cell differentiation. *Nature* **496,** 461–8 (2013).
15. Morris, S. A. *et al.* Dissecting Engineered Cell Types and Enhancing Cell Fate Conversion via CellNet. *Cell* **158,** 889–902 (2014).

16. Liu, Y.-Y. & Barabási, A.-L. Control principles of complex systems. *Rev. Mod. Phys.* **88,** 35006 (2016).
17. Noël, J. P. & Kerschen, G. Nonlinear system identification in structural dynamics : 10 more years of progress. *Mech. Syst. Signal Process.* **83,** 2–35 (2017).
18. Nilsson, R., Björkegren, J., Pena, J. & Tegnér, J. Consistent feature selection for pattern recognition in polynomial time. *J. Mach. Learn. Res.* **8,** 589–612 (2007).
19. Wolfram, S., *A New Kind of Science,.* Wolfram Media, Champaign, IL (2002).
20. Zenil H., Soler-Toscano F., Kiani N.A., Hernández-Orozco S., Rueda-Toicen A., A Decomposition Method for Global Evaluation of Shannon Entropy and Local Estimations of Algorithmic Complexity, arXiv:1609.00110

Supplementary Information

Section 1: Theory and Definitions

Algorithmic causality: The causal content c of a dynamical system S_t running over t is given by the smallest c such that $C(S_t) \geq |S_t| - c$, where $| X |$ denotes the size of X. The difference $|S_t| - C(S_t)$ is an approximation of the causal content c of S_t. The causal content c of a non-causal system approximates log t, i.e. is very small, meaning that $C(S_t) \sim |S_t|$, and that the trajectory of S_t is algorithmic random. For causal systems we have that $C(S_t) - C(S_{t+1}) \sim \log_2 t$, i.e. the complexity of a causal system S is driven only by its evolution time t. All logarithms are in base 2 if not otherwise established.

Algorithmic perturbation analysis: Is the estimation of the effects of perturbations (e.g. by removal/knockout) of an element e (or set of elements) from S, denoted by S\e, on the original algorithmic information content C(S). Without loss of generalization, let's take as a system s, a network G = {V(G), E(G)} as a dynamic system, with V(G) a set of nodes and E(G) a set of links connecting nodes in V(G).

Negative information element (e.g. a node or edge): an element (or set) e in G such that: $C(G) - C(G\backslash e) < -\log_2|V(G)|$, i.e. the removal of e moves G towards randomness.

Positive information element (e.g. a node or edge): an element (or set) e in G such that: $C(G) - C(G\backslash e) > \log_2|V(G)|$, i.e. the removal of e moves G away from randomness.

Neutral information element (e.g. a node or edge): an element (or set) e in G such that e is neither positive or negative:
$-\log_2 |V(G)| \leq C(G) - C(G\backslash e) \leq \log_2 |V(G)|$, where $|V(G)|$ is the size of the system, e.g. the vertex count of a network G.

Algorithmic system inference of its generating mechanism: If $C(S_t) - C(S\backslash e) \sim \log_2 t$ then we call e a neutral perturbation. This means that perturbation e does not compromise the generating mechanism of S and thus S_t can be recovered from $S_t\backslash e$ because $S_{t+1}\backslash e = S_t$, e is disruptive (positive or negative) otherwise with degree of disruptiveness $C(S_t\backslash e) - C(S_t)$. In general, $C(S_t) - C(S_{t-n}) \sim n \log t$ providing the means to reverse a system in time and reveal its possible generating mechanism in the process. If the system is not reversible, a number of generating models may be generated thereby producing optimal hypotheses in the form of generative models.

***Spectra*(G)**: the list of all non-integer algorithmic-information contribution values of each element of G (e.g. edges or nodes, or both).

***Powerset spectra*(G)**: the list of all non-integer algorithmic-information values of each element in the powerset of elements of G (e.g. edges or nodes or both).

Red shifted *spectra*(G): a *spectra*(G) that contains more elements whose removal move G towards randomness than away from randomness.

Blue shifted *spectra*(G): a *spectra*(G) that contains more elements whose removal move G away from randomness than towards randomness.

σ(G): the information signature (or just signature) of G is *spectra*(G) list sorted from largest to smallest value. (see Extended Data Figures. 1-2).

Δ(s): the instantaneous programmability value of an element s in σ(G) indicating how fast or slow s can move G towards or away from randomness**.** Formally,

$$\Delta(s) = | \sigma_i(G) - \sigma_{i-1}(G) / P(\sigma_i(G)) - P(\sigma_{i-1}(G)) |.$$

Information incoherent set: a set whose individual elements or subsets are of different information contribution value than the whole set.

Information coherent set: a set whose individual elements or subsets are of same information contribution value than the whole set.

Information sensitivity: the derivative of the absolute max value of the programmability of a graph in the (re)programmability curve (see Extended Data Figures 1-4). But numerically calculated by the rate of change of σ(G\e) versus σ(G), for all element (or set) e in G, i.e. the list of signatures for all e (or signature of signatures of G) capturing the non-linear effects of perturbations on G.

MILS: Minimal Information Loss Sparsification is a method to identify neutral elements that have zero or negligible algorithmic-information content value in a system or network and can thus safely be removed ensuring minimal information loss.

MAR: a Maximal Algorithmic Random graph (or system) G is an Erdős -Rényi (E-R) graph that is algorithmically random, i.e. whose shortest possible computer description is not (much) shorter than |E(G)|, where |E(G)| is the number of edges of G; or, $|E(G)| - C(G) < c$.

1st Order randomness deficiency: The algorithmic-information distance between a network/system and its algorithmically randomized version, e.g. a MAR graph for networks.

2nd Order randomness deficiency: The difference between information signatures by e.g. Kolmogorov-Smirnoff distance, i.e. how removed a network is from its algorithmic (non-causal) randomization.

Simply directed graph: is the transformation of an undirected graph into a directed one such that the edge directions are chosen to minimize the number of independent paths and number of path collisions.

MAD: denotes the median absolute deviation, and is defined by:

$$MAD = \text{median}(|X_i - \text{median}(X)|).$$

MAD is a robust measure of the variability of a univariate sample.

Relative (re)programmability: $P_r(G) := MAD(\sigma(G))) / n$ or 0 if n = 0, where n = max(|σ(G)|). This index measures the shape of $\sigma_P(G)$ and how it deviates from other distributions (e.g. uniform or normal).

Absolute (re)programmability: $P_A(G) := |\int S(\sigma_P(G)) - \int S(\sigma_N(G))| / m$, where m = $\max(\int S(\sigma_P(G)), \int S(\sigma_N(G)))$ and S is an interpolation function. This measure of reprogrammability captures not only the shape of $\sigma_P(G)$ but also the sign of $\sigma_P(G)$ above and below x = 0.

Programmability landscape: the Cartesian product $P_r(G)$ x $P_A(G)$.

Combined (re)programmability: $||V_R(G)|| = \sqrt{P_R^2(G) - P_A^2(G)} \leq \sqrt{2}$.
The combined reprogrammability is a metric induced by the norm ||V_R (G)|| defined by the Euclidian distance between two (re)programmability indexes. This metric combines the relative and absolute (re)programmability indexes, which takes into equal account both the sign of the signature σ(G) of G and the shape of σ(G), and consequently minimizes the impact of uncertain sign estimations due to (convergent) errors in the calculation of algorithmic complexity[1] due to boundary conditions (see Graph Algorithmic Probability as Upper Bounds to Graph Randomness).

Natural (re)programmability: is the expected theoretical (re)programmability of a system or network, compared to its estimated, e.g. for a complete graph all nodes, and all edges, should have the same algorithmic-information contribution and thus σ(G) can be analytically derived (a flat uniform distribution x = log |V(G)| with |V(G)| the node count of G). A complete graph has thus all its nodes as 'slightly' positive (or more precisely neutral if they are 'positive' by only log |V(G)|).

Algorithmic (Kolmogorov-Chaitin-Solomonoff) Complexity. The theory of Algorithmic Information[2] provides the (ultimate) refinement upon what constitutes to be *a cause (or causal)*. The causal origin of an event gamma is a generating mechanism alpha such that alpha ≠ gamma, and gamma is mechanistically generated/computed from alpha. Formally, the algorithmic complexity[3,4] of a string s is given by C(s|e) := min{|p| : U(p,e) = s}, where p is the program that produces s and halts running on a (prefix-free[5]) universal Turing machine U with input e which can be empty and represented by simply C(s). C (s) is the length of the description of the generating mechanism. An object s is referred to as random and thus non-causal if the algorithmic complexity C(s) of s is about the length of s itself (in bits), i.e. it has no generating mechanism other than a print(s) function. Algorithmic complexity C is the accepted mathematical measure of intrinsic randomness of an object (independent of probability distributions), which is a generalization of statistical randomness and a refinement over the concept of Shannon entropy as it does not depend on choice of probability distribution. Moreover, it has been proven to be mathematically robust (by virtue of the fact that independent definitions converge[4,6,7] unlike the case of Shannon Entropy[1] and because no computable measure can fully characterize (non-statistical) randomness (and therefore causal versus non-causality) due to the lack of universal computational power to test for every possible non-random feature[8]. C can also be seen as a measure of compressibility, but compression algorithms (e.g. LZ, LZW) are rather entropy rate estimators and thus behave exactly like Shannon entropy (Fig. 1j) despite their generalized use as estimators of C.

The *Invariance theorem*[3,4,9] guarantees that complexity values will only diverge by a constant (e.g. the length of a computer compiler, i.e. a translating program between universal reference Turing machines U_1 and U_2) and will asymptotically converge. Formally, $|C(s)_{U1} - C(s)_{U2}| < c$.

C(s) as a function that takes s to the length in bits of the length of the shortest program p that generates s (and halts) is *lower semi-computable*, which means it can only be approximated from above. Proper introductions to the areas of finite algorithmic complexity and applications are provided in[2],and to algorithmic (infinite sequence) randomness can be found in [5,10,11].

Algorithmic Probability

Let U denote a universal machine and let |p| denote the length of a program p. The Halting probability Ω [12] is the probability that U halts for random computer program p constructed bit by bit by random flips of a coin. That is,

$$\Omega_U = \Sigma_{p:\, T \text{ halts on } p}\, 2^{-|p|}$$

Ω is rather a family of probabilities as it depends on the enumeration of programs or reference universal Turing machine U, but optimal choices exist due to invariance-type of theorems [13]. The Algorithmic Probability (AP) [9,13] (also known as Levin's semi-measure or Universal Distribution[14]) of a sequence s is the probability that s is produced by a computer program p, constructed bit by bit by flipping a coin, running on a reference universal Turing machine U divided by their Halting probability. Formally,

$$AP(s) = (1/\, \Omega_U)\, \Sigma_{p:T(p)=s}\, 2^{-|p|}$$

Algorithmic probability allows reaching a consensus of possible explanations of an underlying generating mechanism explaining the system (e.g. a network) at any time thereby providing the most robust hypothesis for the available observable data. Algorithmic probability establishes and shows[15,16] that the consensus of several algorithmically likely solutions is the most likely one.

The chief advantage of algorithmic indices is that causal signals in a sequence may escape entropic measures if they do not hold statistical regularities but they do not escape the metric of AP as there will be a Turing machine T capturing every statistical but also algorithmic aspect of s that compresses s but produces s in full with no less or more information than s itself (thus being lossless).

Numerical approximations to Algorithmic Complexity (C) using Algorithmic Probability (AP)

The Coding Theorem Method (CTM)

Lossless compression has traditionally been used to estimate the algorithmic content of an object s. The algorithmic complexity of a sequence s is then defined as the length of the shortest compressed file producing s when decompressing it (the file must contain the decompression instructions and thus comes always with a natural overhead). While lossless compression is an approximation to algorithmic complexity, actual implementations of lossless compression algorithms (e.g. Compress, Bzip2, gzip, PNG, etc) are purely based upon entropy rate[1,17] and thus can only deal with statistical regularities of up to a window length size, thus not being more related to algorithmic complexity than entropy alone itself. Entropy and entropy rate, however, are not sufficiently sensitive and are not inherently invariant to object description[1,17].

AP, however, constitutes a true algorithmic approach to numerically estimate C(s) by way of the *algorithmic coding theorem* [Levin] formally relating these two seminal measures as follows:

$$C(s) = -\log AP(s) + O(1)$$

The *Coding Theorem Method* (or simply CTM)[15,16] is rooted in the relation between C(s) and AP(s) i.e. between the frequency of production of a sequence and its algorithmic probability. Unlike other computable measures, such as Shannon Entropy, CTM has the potential to identify regularities that are not only statistical (e.g. a sequence such as 1234...), that has as shortest program (and generating model) n:= n+1, that is even sequences with high Entropy but no statistical regularities that are not random, have low algorithmic complexity and are thus causal as the result of an evolving computer program.

As previously demonstrated[15,16], an exhaustive search can be carried out for a small-enough number of Turing machines for which the halting problem is known, thanks to the Busy Beaver game[18]. One strategy to minimize the impact of the choice of T is to average across a large set of different Turing machines all of the same size[15,16]. Let (n, k) be the space of all n-state m-symbol Turing machines, n, k >. Then:

$$D(n, k)(s) = | \{T \text{ in } (n, k): T \text{ produces } s\} | / | \{T \text{ in } (n, k)\} |$$

is the function that assigns to every finite binary sequence s, where T is a standard Turing machine as defined in the Busy Beaver problem[18]. We remark that $0 < D(n, k)(s) < 1$, $D(n, k)(s)$ and is thus said to be a semi-measure, just as AP(s) is because the probability measure does not reach 1 due to non-halting machines. Then using the relation established by the coding theorem [Eq 1], the measure of complexity which is heavily reliant upon AP used throughout this paper can therefore be defined[15,16], as follows:

$$CTM(s, n , k) = – \log_n(D(n, k)(s)) \quad [Eq\ 2]$$

CTM is thus an upper bound estimation of algorithmic complexity[17]. For small values n and k, D(n, k) is computable[19,20] whereas for larger objects the estimation is based on an informed cutoff runtime based on both theoretical and numerical grounds asymptotically capturing most of the halting Turing machines in polynomial time [5,21].

The Block Decomposition Method (BDM)

Because CTM is computationally very expensive (equivalent to the Busy Beaver problem), the algorithmic complexity for only short sequences (currently all up to length k = 12) have thus far only been estimated by the CTM method. To approximate the complexity of a longer sequence is therefore necessary to aggregate the various computer programs that generate the string in a clever fashion by taking advantage of Shannon entropy; the new hybrid measure thus calculates local algorithmic complexity and global Shannon entropy at the same time. Formally, the BDM of a string or finite sequence s is as follows [22]:

$$BDM(s, l, n, k) = \sum_i^j CTM(x_i, n, k) + \log(s_i) \quad [Eq\ 3]$$

where s_i is the multiplicity of x_i, and x_i is the subsequence i after decomposition of s into subsequences x_i, of length l, with a possible sequence remainder y if $|y| < l$ if its length is not a multiple of the decomposition length l. The parameter k runs from 1 to l that CTM can handle, m is an overlapping parameter to deal with the boundary conditions (the remainder sequence). The boundary conditions were studied in [22] where it is shown that BDM errors due to boundary conditions are convergent and vanish asymptotically, and that BDM is lower bounded by Shannon entropy and upper bounded by algorithmic complexity thereby providing local estimations of algorithmic complexity and global estimations of entropy.

Graph Algorithmic Probability as Upper Bounds to Graph Randomness

We have shown that not all measures are robust to object description[1] but that algorithmic probability and algorithmic complexity are up to a constant term[23,34]. An adjacency matrix thus can be taken as the lossless description of a network as it is invariant (up to automorphisms). We look at the algorithmic probability of such a matrix to be produced by a computer program

working on a grid (e.g. a so-called Turmite emulated by a Turing machine) by chance. For every network or graph G, we can therefore estimate the algorithmic information content K(G) based on the likeliness of such adjacency matrix to be produced from an empirical distribution after application of the algorithmic Coding theorem.

The algorithmic complexity K of a graph G is defined as follows,[22,23,34]. Let A(G) be the adjacency matrix of G and Aut(G) its automorphism group, i.e. the set of isomorphic graphs of G to itself, then the algorithmic complexity of the graph is $K(G) = \min\{K(A(G))|A(G) \in A(Aut(G))\}$, where A(Aut(G)) is the set of adjacency matrices for each $G \in Aut(G)$. Since $K(D(G)) \sim K(A(G))$ for any computable lossless description D of G [34] we can safely write K(G) and it can be proven[22] that if G and G' are isomorphic graphs, then $|K(G) - K(G')| < c$, that is they have both similar algorithmic information content. It has been proven using numerical approximations that graphs in large automorphism groups have similar low algorithmic complexity and graphs with small automorphisms groups can have both low and high complexity[23], thereby establishing a one-way numerical relationship between algebraic complexity by group symmetry and algorithmic complexity approximated by BDM with results conforming with the theoretical expectation. Let call such approximation of K(G) with BDM, C(G):

The algorithmic complexity C(G) of graph G is defined by

$$C(G, x_i) = \sum_{(r_i, n_i)} x_i \log(s_i) + CTM(r_i) \qquad \text{[Eq 4]}$$

where set x_i is composed of the pairs (r, n) with r an element of the decomposition of G in square sub-arrays of equal and s_i the multiplicity of each submatrix x_i by using 2-dimensional Turing machines in the calculation of CTM.

Theorem: There exists ER graphs that are not maximal algorithmic random graphs.

Proof: Let p(t) be a binary pseudo-random number generator with seed t shown to produce good statistical randomness. Let G be an ER graph of size n with edge density r. There are therefore $rn(n-1)/2$ edges. Let every edge $e_i \in \{e_1,...,e_{rn(n-1)/2}\} \in G$ be connected to node $v_i \in \{v_1,...,v_n\}$ if p(t) = 1 and disconnected otherwise. G is clearly ER but not maximal algorithmic random because G is recursively generated by p with seed t.

To this date, there were no alternatives to apply non-linear interventions to complex systems in the phase space other than to actually simulate dynamical trajectories of a system assumed on little to no knowledge or assume them to be linear and in fixed points, and even so requiring computationally intractable resources. This new calculus, however, requires much less information to provide educated causal interventions promising to be useful and powerful.

Algorithmic-information Causal Interventional Calculus

The core of the causal calculus is based upon the change of complexity of a system subject to perturbations, particularly the direction (sign) and magnitude of the difference of algorithmic information content C between two graphs G and G', e.g. the removal of e from G (denoted by G\e). The difference $|C(G) - C(G\backslash e)|$ (see Supplement, Section 1) is an estimation of the shared algorithmic mutual information[1] of G and G\e. If e does not contribute to the description of G, then $|C(G) - C(G\backslash e)| \sim \log_2|V(G)|$, where |V(G)| is the node count of G, i.e. the difference will be very small and at most a function of the graph size and thus C(G) and C(G\e) have almost the same complexity. If, however, $|C(G) - C(G\backslash e)| < \log_2|V(G)|$ bits, then G and G\e share at least n bits of algorithmic information in element e, and the removal of e results in a loss of information. In contrast, If $C(G) - C(G\backslash e) > n$, then e cannot be explained by G alone nor is it

algorithmically not contained/derived from G, and it is therefore a fundamental part of the description of G with e as a generative causal mechanism in G, or else it is not part of G but has to be explained independently , e.g. as noise. Whether it is noise or part of the generating mechanism of G depends on the relative magnitude of n with respect to C(G) and to the original causal content of G itself. If G is random then the effect of e will be small in either case, but if G is richly causal and has a very small generating program, then e as noise will have a greater impact on G than would removing e from the description of an already short description of G. However, if $| C(G) - C(G\backslash e) | \leq \log_2 |V(G)|$, where $|V(G)|$ is the vertex count of G, then e is contained in the algorithmic description of G and can be recovered from G itself (e.g. by running the program from a previous step until it produces G with e from G\e).

For example, in a complete graph K_{10} (Fig. 1a,b), the removal of any single node leads to a logarithmic reduction in its algorithmic complexity, but the removal of any single edge leads to an increase of randomness. The former because the result is simply another complete graph of a smaller size, and the latter because the deleted link would need to be described after the description of the complete graph itself. However, the removal of node 1 (Fig. 1 b) is equivalent to the removal of the set of all edges connecting to node 1, so the set of all these edges is a positive information set even though all its individual edges are negative, a nonlinear phenomenon that we call *information incoherence*. Connecting two complete graphs at a random node (Figure 1c) designates the connecting link as positive because its removal pushes the network towards simplicity, the minimal description of 2 K_{10} graphs being shorter than the minimal description of 2 K_{10} graphs plus the description of the missing link at random points. Such a link can also be seen as an element connecting 2 networks, hence a network of networks. Its identification and removal would thus reveal the separation between two networks. In general, positive elements will identify the major structures generated by the most likely (and simplest) generating mechanism given the observation, and odd elements will stand out as negative, thereby identifying layers of networks that are independent of separable generating mechanisms, even removing apparent noise (external information) from the signal (the system's natural evolution) when such networks are richly causal. Random graphs are node- and edge-*blueshifted (see Fig. 1g)*—; simple graphs such as complete or wheel graphs are edge-*redshifted*. Perturbing (e.g. knocking-out) a node and recalculating the spectra changes the original spectrum in what is clearly a non-reductionistic approach to characterizing networks. All the methods introduced here also work on directed (e.g. Fig. 1d) and weighted graphs without any loss of generality.

Real-world networks as generated by physical laws are recursive according to classical mechanics (deterministic and reversible), and are thus on the left side in the schematic Extended Data Figure. 1, but they may also contain information about other interacting systems or be captured in a transient state that incorporates external signals pushing the networks towards randomness. We have quantified this concept by proposing different (Re) Programmability indices (see Supplement Section 1). Extended Data Figure. 1 summarizes some of the theoretical expectations and numerical results. The curve is negatively skewed because of a thermodynamic argument: while it is easy and fast to move regular networks towards randomness as a function of the number of edges—there being about $|E(G)|$ ways to move the network towards randomness such that the description of G moves to $|G| + |e|$, i.e. the description of, say, an edge removed, where $|E(G)|$ is the edge count of G-- there are far fewer ways to move a random network away from randomness. A MAR graph, for example, cannot be moved by edge or node deletion more than $\log |E(G)|$. The result is compatible with

the asymmetries in energy landscapes between moving systems towards fewer future attractors versus moving them back to states of a greater number of attractors, the latter requiring much more energy than the former.

Minimal Information Loss Sparsification (MILS)

Our causal algorithmic calculus defines an optimal parameter-free dimension reduction algorithm, which minimizes information loss while reducing the size of the original (network) object. The Minimal Information Loss Sparsification (or MILS) method is based on removing neutral elements while preserving the information content of a network, and therefore its properties, and it can be used for reduction by minimizing the loss of any informational feature of G that needs to be described and cannot be compressed into some shorter description of G (see Supplement Section 2 for the pseudocode and evaluation).

Maximal Algorithmic Randomness Preferential Attachment (MARPA) algorithm

The Maximal Algorithmic Randomness Preferential Attachment (MARPA) algorithm (MARP) (see Supplement Section 2 for the pseudocode and evaluation) can be viewed as a reverse algorithm in comparison to MILS. MARPA seeks to maximize the information content of a graph G by adding new edges (or nodes) at every step. The process approximates a network of a given size that has the largest possible algorithmic randomness and is also an Erdős-Rényi (ER) graph. An approximation of a 'Maximal' Algorithmic- Random (MAR) graph can be produced as a reference object whose generating program is not smaller than the network (data) itself and can better serve in maximum (algorithmic-) entropy modelling. See Supplement Section 1 for the proof of the existence of ER graphs that are not maximal algorithmic-random graphs

Dynamical simulations using Boolean networks

We conducted a first experiment: single-node and single-edge deletion effects on all possible Boolean networks with XOR, AND, and OR as functions with up to the size of 5 nodes. A Boolean network consists of a discrete set of Boolean variables each of which has a Boolean function (here, always the same for each node), which takes inputs from a subset of those variables. The output of a Boolean network is the state of the numbered sequence of states of its nodes. In a Boolean model in which a network is represented by a set of N Boolean variables, either Off (0) or On (1), the number of attractors cannot exceed 2^{n2^n}.

In general, in a connected network, each node is controlled by a subset of other nodes. The size of the controlling subset for each network depends on the connectivity pattern in the network [3, 4]. For example, in an E-R random graph with edges equally distributed with edge density p, if we change the state of any arbitrary node in the initial state, the effect on the dynamics of a network should be about the same on average, and this means the basin of attraction remains mostly unchanged. If the basin of attraction is of size M, the number of attractors is $(2^n)/M$. The size of M will depend on the network density p with $M<<2^n$. However, in a simply connected complete graph, all other nodes control all nodes and there is only one attractor with basin of attraction size 2^v. In modular scale-free networks, not all edges are statistically equally distributed and few nodes control many others, unlike an E-R random network, and they show significantly greater basins of attraction sizes and therefore have a smaller number of attractors[2–4].

We estimated the algorithmic-information contribution of every node n (and every edge e) over all possible 33,554,432 5-node graphs. The estimation of the algorithmic-information contribution (see Supplement Section 1)) considered all vertices in the same orbit of the automorphism group of G, Aut(G), and the min of the information value C(G\n) with respect to the largest component of G according to the unlabelled definition of algorithmic complexity for unlabelled graphs in [2], thus correcting minor deviations of estimations of the complexity of C(G\n) by BDM due to boundary conditions [1]. The calculation of C(G') for every G' in Aut(G) is, however, not feasible in general as the production of Aut(G) and thus the calculation of C(G') for all G' in Aut(G) is believed to be in NP, thereby making the brute force exploration computationally intractable (in [2 and 3]. However, it has also been shown that estimations of K(G) are similar to K(Aut(G))).

We performed the same edge perturbation experiments, removing all edges, one at a time, from larger graphs, [Fig3e] and comparing with state-of-the-art algorithms [4] the largest eigenvalue, number of different eigenvalues and number of attractors on the largest remaining connected component of the larger graphs. The experiment was repeated with Boolean functions OR, XOR and AND, leading to the same results.
One can then apply uninformed perturbations to move networks towards statistical randomness based on this algorithmic-information calculus, and in a controlled fashion towards and away from algorithmic randomness, thus taking into account non-statistical and non-linear effects of the system as a generating algorithmic mechanism, providing a sequence of causal interventions to move networks and systems at the level of the (hypothesized) generating model in order to reveal first principles and to control the side effects of such a system's manipulation at every step.
Random versus regular networks are sensitive in different ways. While an algorithmic- random network is hard to move fast along its algorithmic -random location (Extended Data Fig. 1-4), other changes in simple regular graphs have more dramatic effects (Fig1a v Fig1c), displaying different degrees of linear v. non-linear behaviour for different perturbations. In low algorithmic-content networks such as *simply directed complete graphs*, all nodes are immune to perturbations, leaving the basins of attraction and number of attractors the same (only proportional to their new size). From these principles, it is evident that systems that are far from random display inherent regular properties, and are thus more robust in the face of random perturbations because they have deeper attractors (See Supplement Section 2).

Algorithmic Causal Reconstruction of Dynamic Systems
The theory of algorithmic complexity provides means to find mechanistic causes through most likely (simplest) algorithmic models, helping to reverse engineer partial observations from dynamic systems and networks.
The causal reconstruction method of a system (e.g. a network or cellular automaton) M is as follows:

1) Estimate the information contribution of every element e in O(n), the sequence of instantaneous observations O from time 0 to n.
2) The set of neutral elements {e} is the set of those elements whose algorithmic-information content contribution to the complexity O(n) is of a logarithmic nature only with respect to C(n).
3) Remove neutral elements {e} from O(n) and repeat (1) with reassigned O(n) := O(n)\{e}.
4) After m iterations the reverse sequence of observations O(n)\{e} provides an indication of the evolution of the system in time, thereby yielding a hypothesis about the

generating mechanism P producing O(n) for any n, and unveiling the initial condition in the last element of the above iteration, or the first after reversing it (see supplement, section 2 for more details and an example).

SI SECTION 1 REFERENCES

1. Chaitin, G. *Algorithmic Information Theory*. (Cambridge University Press, 1987).
2. Wuensche, A. in (eds. Wagner, G. & Schlosser, G.) 1–17 (Chicago University Press, 2004).
3. Espanés, P. M. De, Osses, A. & Rapaport, I. BioSystems Fixed-points in random Boolean networks : The impact of parallelism in the Barabási – Albert scale-free topology case. *BioSystems* **150,** 167–176 (2016).
4. Aldana, M. Boolean dynamics of networks with scale-free topology. **185,** 45–66 (2003).

Section 2: Parameter-free Algorithms: pseudo-codes and evaluations

Dynamical simulations using Boolean networks

We first explored whether the algorithmic content, or more precisely the information spectrum, of a system/network, influences transitions between different stable states thereby effectively providing a tool to steer and reprogram networks. We observed an average decrease of size of reachable states for all nodes (mean value), and the distribution of reachable states becomes more clustered (standard deviation), and more symmetrical (skewness) for all graphs with 5 nodes and single deletion. Positive info nodes had a similar effect as a deletion of a hub in the network. Absolute and relative negative have similar effect, whereas neutral (no information change) nodes preserve the distribution skewness closest to original.

Histograms of perturbation effects on all graphs of size 5 nodes using functions XOR, AND, and OR produced similar results (see Fig3d & raw data infoedgesmotifs5.csv). Due to the small size of the graph we were able to control for graph automorphisms to correct minor BDM errors produced by boundary conditions[22]. Two objects x, y are in the same orbit if there is an automorphism φ in Aut(G) such that $\varphi(X) = Y$ (equivalently, $X = \varphi^{-1}(Y)$). In the algorithmic perturbation analysis, if elements $e_1, \ldots, e_n$ in E are in the same orbit in Aut(G) we take as the perturbation of every element in E to be all equal to $\min\{| C(G\backslash e_1) - C(G) |, \ldots, | C(G\backslash e_n) - C(G) |, \ldots\}$. In other words, the effect of every element e_i in E on G is the same. The automorphism group Aut(G) was generated with help of public software[24,25] for this experiment. For larger networks, however, this becomes computationally expensive in the context of the perturbation analysis and thus, because we have shown that $K(G) \sim K(Aut(G))$[34], we continued calculating C(G) only.

In the exhaustive experiment over all connected graphs of node count 5, deleting the largest versus smallest node degree produced statistical differences as expected as previously suggested[26]. More relevant to our purposes, it was found that positive versus negative versus neutral information node/edge removal led to statistically different effects when executed in connected networks. Negative information node removal was interestingly not similar to lowest degree removal, yet statistically significant different to control (random) node removal. Absolute and relative negative information removal had similar effects, and neutral (no information change) nodes/edges kept the distribution skewness closest to the original distribution, in concordance with theory. For negative edges, the number of attractors was significantly increased (Fig3d) as the theory predicted.

Minimal Information Loss Sparsification (MILS)

Below we provide the pseudo-code for the MILS algorithm. MILS allows dimensionality reduction of a graph (or any object) by deletion of neutral elements, thus maximizing preservation of the most important properties of an object as the algorithmic information content is invariant under neutral node perturbation. Let G be a graph, then:

1. Calculate the *powerset spectra*(G) and let E_j be the subset j in the set of all non-empty proper subsets of edges $\{e_1, \ldots, e_n\}$ in G.
2. Remove the subset E_j such that $C(G\backslash E_j) < |C(G\backslash E_i)|$ for all E_i in *powerset spectra*(G), where |C| is the absolute value of C.
3. Repeat 1 such that $G := G\backslash E_j$ until final target size is reached.

The algorithm time complexity class is in $O(2^{p(n)})$ (if there are no subsets with same information

value) because of the combinatorial explosion of the power set, but a more efficient suboptimal version of MILS iterates over only singletons:

1. Calculate $G\backslash e_i$ for all $i \in \{e_1,...,e_n\}$ i.e. *spectra*(G).
2. Remove edge e_j in *spectra*(G) such that $C(G\backslash e_j) < |C(G\backslash e_i)|$.
3. Repeat 1 with $G := G\backslash e_j$ until final target size is reached.

We call e_j a neutral information edge because it is the edge that contributes with less information content (in particular, minimizes information loss or introduction spurious information) to the network according to the information difference when removed from the original network.
Assuming that the estimations of C(G) and *spectra*(G) are definite and fixed (in reality one can always find tighter upper bounds though due to C's semi-computability), and MILS is a deterministic algorithm. Let G be a network and $i(e) = C(G) - C(G\backslash e)$ be the information value of element e in G with respect to G. If $i(e') > i(e)$ then MILS algorithm removes e first (by definition) because it minimizes the loss of information if the choice is to remove either e or e'. We have thus that $C(G\backslash e_1) = C(G\backslash e_2)$ if, and only if, $i(e_1) = i(e_2)$. However, it does not hold in general that $C(G\backslash e_1\backslash e_2) = C(G\backslash e_2\backslash e_1)$, that is, the removal of e_1 followed by the removal of e_2 from G, is not equal to the removal of e_2 followed by the removal of e_1 from G, even for $i(e_1) = i(e_2)$ because of non-linear effects (i.e. the removal of e_i may modify the information contribution of all other e_j in $G\backslash e_i$)**.** This suggest that the only way to deal with these cases for MILS to be deterministic is the simultaneous removal of the set of elements $\{e_1, \dots e_n\}$ such that $i(e_1) = \dots = i(e_n)$. The time complexity of MILS thus ranges between the original $O(n^2)$ in the worst case to O(1) when all nodes have the same information value/contribution to G and are thus removed in a single step. Therefore, set removal turns MILS into a proper deterministic algorithm that yields the same object for any run of MILS over an object G. Because any property of a network ultimately contributes to its information content (the amount of information to describe it), information minimization will preserve any potential measure of interest. We show in the following section that minimizing loss of information maximizes the preservation of graph theoretic properties of networks such as edge and node betweenness, clustering coefficient, graph distance, degree distribution and finally information content itself.

Experimental evaluation of MILS using real-world networks

Depicted in Fig1(i) and (j), an example of a scale free network with 100 nodes and its original *information signature* (see Supplement section 1) which after neutral edge removal preserves the information signature (by design) after deleting 30 neutral edges but also preservation of graph theoretic properties such as edge betweenness, clustering coefficient and node degree distribution after deleting all graph edges better than several other common sparsification methods (validated on 20 other gold-standard networks ([27] & see Supplement Section 1). This is because an element that is deleted will lead to a reduction of its algorithmic information content, so in the maximization attempt to preserve its algorithmic information content only the less informative or most redundant properties of a network/system will be removed.
When MILS is applied to a set of well-known networks used before in pioneering studies [27] we find that not only the loss information signatures and thus the non-linear algorithmic information content of the system was minimized, but also that all the tested and most common graph-theoretic measures are maximally preserved versus random deletion and other common dimension reduction methods .

Maximal Algorithmic Randomness Preferential Attachment (MARPA) algorithm

MARPA allows constructions of a maximally random graph (or any object) by filling out the blanks, i.e. adding edges, for any given graph in such a manner that randomness increases. Let G be a network and C(e) the information value of e with respect to G such that C(G) – C(G\e) = n. Let P = {p_1, p_2, …, p_n} the set of all possible perturbations. P is finite and bounded by $P < 2^{|E(G)|}$ where E(G) is the set of all elements of G, e.g. all edges of a network G. We can find the set of perturbations e' in P such that C(G) – C(G\e') = n' with n' < n. As we iterate over all e in G and applying the perturbations that make n' < n, for all e, we go through all $2^{|E(G)|}$ possible perturbations (one can start by all |E(G)| single perturbations only) maximizing the complexity of G' = max{G | C(G) – C(G\e) = max among all p in P and e in G}. Alternatively, there is a configuration of all edges in G that maximizes the algorithmic randomness of G, let such a maximal complexity be denoted by maxC(G), then we find the sequential set of perturbations {P} such that maxC(G) - C(G) = 0, where C(G) - maxC(G) is a measure related to randomness deficiency[28,29] of how removed G is from it (algorithmic-) randomized version maxC(G) (notice that C(G) is upper bounded by maxC(G) and so the difference is always positive). Fig. 3a-c, shows how we numerically (single-element wise) moved a regular network towards randomness (in particular an E-R graph). Notice that while an ER network with edge density 0.5 is of maximal entropy, it can be of high or low algorithmic randomness, i.e. recursively generated or not[1] but a high algorithmic random graph is also ER because, if not, then by contradiction it would be statistically compressible and thus non-algorithmic random, this is because a graph with any statistical regularity would also not be algorithmic random nor ER. One can also consider the absolute maximum algorithmic random graph, denoted by amaxC(G) and disconnected to the number of elements of G (thus not a randomization of G), that is the graph of same number of nodes, but edge arrangement such that $C(G) < C(amax(G)) \leq 2^k$ where $k = (|E(G)|(|E(G)|-1))/4$ is the maximum number of edges in G divided by 2 (at edge density 0.5 reaches max algorithmic randomness. The process approximates a network of some size that has the greatest possible algorithmic randomness and is also an Erdős-Rényi (ER) graph. The pseudo-code is as follows:

1. Start with graph G (can be empty).
2. Attach edge e_j to edge e_j' in G such that $C(G \cup e_j') > C(G)$.
3. Repeat 1 with $G := G \cup e_j'$ until final target size of graph is reached.

Generating a MAR graph is computationally very expensive with exponential time complexity in $O(2^{n^2})$ because at every step all possible attachments have to be tested and evaluated (i.e. all possible permutations of the adjacency matrix of size n × n), but small MAR graphs are computationally feasible, and they represent approximations of "perfect" ER random graphs, that unlike some ER graphs they cannot, in principle, be recursively generated with small computer programs. The intuition behind the construction of a MAR graph is that the shortest computer program (measured in bits) that can produce the adjacency matrix of the MAR graph, is of about the size of the adjacency matrix and not significantly shorter, thus it can in some strict sense it can be considered the perfect ER graph. Every time that a larger graph, and therefore the addition of new edges, is needed, the computer program that generates it grows proportionally to the size of the adjacency matrix (See Supplement section 1 for algorithm and more details).

Algorithmic Causal Reconstruction of Dynamic Systems

In general, observers (see Fig2a) have only limited access to any system's generating mechanism denoted by P or to the precise dynamics D of the same system. To each system's perturbation,

or observation O(n), in time 0 to n, can correspond to an estimation of the complexity C(n) of O(n) based upon the likelihood of P to explain O(n). The objective when attempting to identify a system is access P by inspecting the system at observation intervals (or the consequences of system perturbations) capturing possible features to associate with P. Because knowledge about D, the dynamics governed by a system e.g. ODEs or a discrete mapping such as a cellular automaton, is as a rule beyond reach, network-based approaches can conveniently focus on the relationships among a system's elements represented by a timeline T, thus serving as a topological projection of the system's dynamics based on e.g. correlation (apparent row-column correlation from an observation in time).

Computer programs with empty inputs can encode both the dynamics and changing initial conditions of a system over time, constituting a true causal generating mechanism for all system's timelines, see Fig. 2a, where dynamics and topology are included. Not all systems are equally dependable of their internal kinetic dynamics. For example, network-rewriting systems updated according to replacement rules have no dynamics (See Fig2d). On the other hand, there are systems whose internal kinetics fully determines the system's behaviour i.e. attractor structure, such as Hopfield networks[30] and Boltzmann machines[31], which is independent of their fixed topology (complete graphs). Other networks are, however, more dependent on topology or geometry (e.g. disease networks or geographical communication networks). Boolean networks, governed both by their topological and internal kinetic properties as encoded by the connectivity of the node with the assigned Boolean function[32,33] to that very node. Each observation of a system is necessarily only a partial snapshot of the system's trajectory in phase space and it reveals only certain aspects of the generating cause, yet without any loss of generality one can use the causal calculus here introduced either on T, D or a combination of T and D in order to produce algorithmic models of causal generating mechanisms approaching P and producing T and D. While the focus of the causal calculus here introduced focuses on T, it can readily incorporate D by moving to the phase space without any essential modification and for which we have included some examples using discrete dynamics systems such as cellular automata to show how the same calculus can be utilized. The same elements in D that move a system towards, or away, from randomness are, conversely, positive and negative elements like those defined for T (See Fig2a,b,c,d) in the application to networks.

Reverse-engineering discrete dynamical systems from disordered observations*:*

A cellular automaton (CA) is defined by a rule for computing the new value of each position in a configuration based only on the values of cells in a finite neighborhood surrounding a given position. Commonly a CA evolves on a square grid or lattice of cells updated according to a finite set of local rules which are synchronously applied in parallel. A snapshot in time of the symbols of the cells is called a configuration. A snapshot in space and time (the characteristic CA grid) is called an evolution.

A local and a global function f and λ can therefore define a cellular automaton. Let S be a finite set of symbols of a cellular automaton (CA). A finite configuration is a configuration with a finite number of symbols, which differs from a distinguished state b (the grid background) denoted by $0^{\infty}b0^{\infty}$ where b is a sequence of symbols in S (if binary then S = {0, 1}). A stack of configurations in which each configuration is obtained from the preceding one by applying the updating rule is called an evolution. Formally, Let $f : S^Z \rightarrow S^Z$ where Z is the set of positive integers and n, $i \in N$ then $f(r_t) = \lambda(x_{i-r} \ldots x_i \ldots x_{i+r})$, where f is a configuration of the CA and r_t a row with $t \in N$ and r_0 the initial configuration (or initial condition). The function f is also called the global rule of the CA, with $\lambda : S^n \rightarrow S$ the local rule determining the values of each cell and r the neighborhood

range or radius of the cellular automaton, that is, the number of cells taken into consideration to the left and right of a central cell x_i in the rule that determines the value of the next cell x.
All cells update their states synchronously. Cells at the extreme end of a row must be connected to cells at the extreme right of a row in order for f to be considered well defined. The function λ indicates the local state dependency of the cellular automata and f updates every row. Depicted (Extended Data Figures 7-13) is the Elementary Cellular Automaton (ECA) rule 254 (in Wolfram's enumeration[19]) that generates a typical 1-dimensional cone from the simplest initial condition (black cell) running downwards over time for 20 steps. ECA are CA that considers only the closest neighbors to the right and left and itself therefore 3 cells each with a binary choice for λ. Every ECA such as rule 254 can thus be seen as a 2^3 = 8-bit computer program represented by its rule icon representing its function f (Fig1a P(t)) or a function determining its local and global dynamics (Fig. 2 D(t)). Any perturbation to the simple evolution of the rule leads to an increase of its complexity because a rule with a longer description than rule 254 would be needed to incorporate the introduced random perturbation (blue rows), thus every row in rule 254 is information negative except for the random rows whose deletion would bring the rule to its simplest description (rule 254). Unlike the rest of the dynamic system, the last step in the evolution of a dynamic system is information neutral because it does not add or removes any complexity, so removal of neutral elements reverses the system's unfolding evolution to its original cause (the black cell) and the rule can be derived by reversing the sequence of the neutral elements at every step, effectively peeling back the dynamic system from a single instantaneous of a sequence of observations (in optimal conditions, e.g. no noise and full accuracy, and good enough approximations of algorithmic-information content).
When clustering consecutive rows of the evolution of all Elementary Cellular Automata (256 rules) we found that the later the perturbations in time the more neutral thus conforming to the theoretical expectation (Fig. 3 and Extended Data Figure 7). When taking a sample of representatives ECAs this was also clearly the case (Figure 3). We proceeded to reverse engineer the rule of an ECA by:

1) Produce the space-time diagram O(n) of an ECA from time 0 (initial condition) to time n.
2) Scramble the observations from O(n) (worse case of an observation, to loose track of their order)
3) Sort the scrambled observations to maximize algorithmic probability to find the most likely generating mechanism (with lowest algorithmic complexity).
4) From 2 and 3 estimate the algorithmic-information content of every (hypothesized) step.
5) Compare among all them and sort from lowest contribution to highest.
6) Find the initial condition and generating rule by reversing the order of the sequence of neutral elements from O(n).

Finding the lowest complexity configuration of disordered observations and above we show how we found the correct times, thus providing a most powerful method to reverse engineer and find design principles and the generating mechanism of evolving systems. Running the sequence forward one can also make predictions of the phase space configuration of the dynamic evolving system. Fig. 3 and Extended Data Figure 7 shows that the predicted point in the phase space does not diverge from the actual position of the system in phase space, thus providing good estimations of the evolution of the system both backward and forward.

In what follows in the paper, we choose to work at the level of T for the same convenient simplifying reasons followed by other network-based approaches, but unlike other possible

approaches, the theory and methods holds in general for non-linear dynamical systems and not only static or evolving networks. When working on T only, we assume that lossless descriptions are of the observations (e.g. only T) and not of full descriptions of T and D or even P (the true generating mechanism, e.g. a computer program P) that is the unknown. To this date, there were no other alternatives to apply non-linear interventions to complex systems in the phase space other than to actually calculate dynamical properties of a system often assumed with little knowledge or assumed to be linear and in fixed states, requiring computationally intractable simulations. This new calculus, however, requires much less information to make educated causal interventions proving to be extremely useful and powerful.

Entropy-deceiving graphs

We introduced a method[1] to build a family of recursive graphs of which one is denoted by 'ZK' with the property of being recursively constructed and thus of low algorithmic (Kolmogorov-Chaitin-Solomonoff) complexity (and thus causal) but would appear statistically random and thus as having maximal Entropy for an uninformed observer. These graphs were proven to have maximal Entropy for some lossless descriptions but minimal Entropy for other lossless descriptions of exactly the same object, thereby demonstrating how Entropy fails at unequivocally and unambiguously characterize a graph independent of a particular feature of interest reflected in the choice of natural probability distributions. A *natural probability distribution* of an object is given by the uniform distribution suggested by the object dimension and its alphabet size. For example, if a graph G is losslessly (with no loss of information) described by its adjacency matrix M, then in the face of no other information, the natural distribution is the probability space of all matrices of dimensions |M| and binary alphabet. If, however, G is losslessly described by its degree sequence S with no other information provided about G, the natural distribution is given by probability space of all sequences of length |S| and alphabet size |{S}|, where {S} denotes the number of n-ary different symbols in S. The natural distribution is thus the less informative state of an observer with no knowledge about the source or nature of the object (e.g. its recursive nature). We denote by 'ZK' the graph (unequivocally) constructed as follows:

1. Let 1 → 2 be a starting graph G connecting a node with label 1 to a node with label 2. If a node with label n has degree n, we call it a *core node*, otherwise, we call it a supportive node.
2. Iteratively add a node n + 1 to G such that the number of core nodes in G is maximized.
3. The resulting graph is typified by the one in Fig2d.

Clearly supporting nodes are always the latest to be added at each iteration, perturbing elements of the network other than the last elements will break the generating program and thus these elements will move the network towards randomness whereas removing the latest nodes has little to no impact because it only moves the network back in time, but the originating program remains the same and only needs to run again to reach the same state as before. Thus by inspecting elements that do not contribute or make the network slightly more simpler one can reverse the network in time thereby revealing its generating mechanism (See Algorithmic Causal Reconstruction of Dynamic Systems subsection).

We have shown that Entropy is highly observer dependent even in the face of full accuracy and access to object lossless descriptions. These specific complexity-deceiving graphs for which Entropy produce disparate values when the same object is described in different ways (thus with different underlying probability distributions), even when the descriptions reconstruct

exactly the same, and only the same, object. This drawback of Shannon Entropy ultimately related to its dependence of distribution is all the more serious because it is especially overlooked for objects other than strings, such as graphs. For an object such as a graph, we have shown that changing the descriptions does not only may change the values but divergent contradictory values are produced. This means that one not only need to choose a description of interest to apply a definition of Entropy, such as the adjacency matrix of a network (or its incidence or Laplacian) or its degree sequence, but as soon as the choice is made, Entropy becomes a trivial counting function of the feature, and only the feature, of interest. In the case of, for example, the adjacency matrix of a network (or any related matrix associated to the graph such as the incidence or Laplacian matrices), Entropy becomes a function of edge density, while for degree sequence Entropy becomes a function of sequence normality. Entropy can thus trivially be replaced by such functions without any loss but it cannot be used to profile the object (randomness, or information content) in any way independent of an arbitrary feature of interest. The measures introduced here are robust measures of (graph) complexity independent of object description based upon the mathematical theory of randomness and algorithmic probability (that includes statistical randomness), which are sensitive enough to deal with causality and provide the framework for a causal interventional calculus.

Section 3: Evaluation and validation of the causal calculus using transcriptional data and genetic regulatory networks.

E-Coli Transcription Factor Network Ontology Enrichment Analysis

We estimated the information node values of a highly curated E. coli transcriptional network (only experimentally validated connections) from the RegulonDB (http://www.ccg.unam.mx/en/projects/collado/regulondb). Info values were clustered into 6 clusters by using partitioning around K-medoids and optimum average silhouette width. Gene clusters were tested for enrichment of biological functions according to Gene Ontology, KEGG and EcoCyc databases, using topGO "weight01" algorithm for GO or hypergeometric enrichment test for KEGG and EcoCyc. BDM values did not correlate with degree distribution, compression or Shannon entropy. The numerical results suggest that more positive information genes in E-Coli are related to homeostasis processes while more negative info genes are related to processes of specialization, in agreement with the idea that cellular development is an unfolding process in which core functions are algorithmically developed first than more specialized enabling training-free and parameter-free gene profiling and targeting. Extended Figures 8-16 show that other measures fell short at producing statistically significant groups for a gene ontology analysis, and also provides details of the found clusters and elements in them.

Information spectral and enrichment analysis of Th17 differentiation

We applied our method to a dataset on differentiation of T-helper 17 (Th17) cells[35]. Th17 cells are one of the major subsets of T-helper cells, which in addition to Th17 comprise several sub-types such as Th1, Th2 and Treg cells. These subsets all differentiate from a common naïve CD4+ T cell precursor cell type based on environmental signals and are classified by certain lineage-defining markers. Th17 cells are necessary to protect the host from fungal infections, but at the same time are involved in the pathogenesis of several autoimmune diseases, hence the processes driving Th17 differentiation are of great interest to the scientific community[36]. From the gene ontology analysis taking the experimentally known genes involved in the process of differentiation from T naïve to Th17 (Fig. 4e), it is shown that exactly those genes are distributed non-uniformly and in different ways along the 3 time points thereby suggesting that the

algorithmic perturbation analysis succeeds at identifying such genes (otherwise, the distributions would have appeared uniform in all cases).

Information spectral analysis

The information spectral analysis used a reconstructed regulatory network from functional perturbation and transcriptional data corresponding to the Th17 differentiation. The data was divided into three time windows; 0.5 to 2 hours, 4 to 16 hours, and 20 to 72 hours, here referred to as EarlyNet, IntermediateNet and FinalNet respectively. We were interested in investigating whether genes with strongly negative or positive information values would include genes knows to be crucial in Thelper cell differentiation and/or novel putative Th17 regulators, and whether those genes would according to our predictions change their information content throughout the Th17 differentiation process. We noted that in general, genes classified as having the most positive or negative information values covered several genes known to be involved in T cell differentiation such as transcription factors from the IRF or STAT families (see Extended Data Figure 5). The genes assigned in the Th17 regulating modules[35] were present along the spread of information values with some enrichment at extreme positive values. However, not all genes with extreme information values were identified in the original study[35] suggesting that our method may identify additional regulators (Extended Data Figure 5). When analyzing those genes that are present in all 3 networks and determining their evolution over time (Extended Data Figure 5), we noted that genes for chemokines/chemokine receptors were switching from negative values in EarlyNet to positive values in FinalNet. In the gene group switching from positive in EarlyNet via negative in IntermediateNet back to positive in FinalNet, many transcription factors from the STAT family were represented. Extreme (mostly positive) information values were assigned for many members of the IRF family of transcription factors, which comprises well-known regulators of Thelper differentiation (Extended Data Figure 5), including Th17-inhibiting roles for IRF8 which appears on top of the lists in IntermediateNet and FinalNet (Extended Data Figure 5). Only three genes were assigned negative information values in FinalNet, namely STAT6, TCFEB and TRIM24, suggesting that removing these might be able to enhance the Th17 profile.

Clustering

The networks were clustered using the k-means algorithm with 5 clusters per network (Extended Data Figure 5). The list of genes that changed from most negative information values in EarlyNet (cluster 5) towards most positive information values in FinalNet (cluster 1) contained several genes involved in T helper cell subset differentiation and function, for example, HIF1a, FOXO1, IKZF4, IL2, IL21, IL2RA, IL6ST. Conversely, the list of genes with highest information values in EarlyNet overlapping with lowest information values in FinalNet was more restricted in number and contained some general transcription factors such as RelA and Jun.

We noted that in general, genes classified as having the most negative or positive information values comprised many genes known to be involved in T cell differentiation, such as transcription factors from the IRF or STAT families, chemokine receptors, cytokines and cytokine receptors; this was particularly evident for networks 1 and 3. When analyzing those genes that have negative information values in network 1 and change towards positive information values in network 3, we found that the common elements in both lists contain several such genes involved in T helper cell subset differentiation and function, for example, HIF1a, FOXO1, IKZF4, IFNg, IL2, IL21, IL2RA, IL6ST, CXCL10, CXCR3, CXCR5. Interestingly, the list of genes with positive information values in network 1 or with negative information values in network 3 was much more restricted in number and did not overlap, yet contained highly interesting genes. In

network 1, these were mostly transcription factors including several IRFs, STATs as well as RUNX1 and SMAD2, all known to be important in T cell differentiation. The few genes with negative information values in network 3 were STAT6, TCFEB and TRIM24 (interestingly these 3 genes, STAT6, TCFEB, TRIM24 are amongst the few ones centered around 0, i.e. neutral, in network 1), and it is tempting to speculate that over-activation of these might be able to reprogram differentiated Th17 cells to another lineage. Indeed, STAT6 is a well-known factor in IL-4 response and Th2 induction. Notably, in network 2, which may be viewed as a transition state, 3 genes were assigned the most positive information values and all of these belonged to the IRF family of transcription factors, which comprises well-known regulators of Thelper differentiation, including Th17-inhibiting roles for IRF8 which appears in said list.

Enrichment Analysis

To assess to what extent our informational spectral analysis identifies genes, which are relevant to the differentiation process in Th17 cells we perform an enrichment analysis based on a literature survey. To this end we collected 9 landmark papers in the Th17 literature [35,37–44]. From each paper a list of genes is extracted (manually), trying to select the set of genes, which the text identifies as relevant for Th17 differentiation. The script calculates all the intersections between these sets, genes in a greater number of intersections is given a higher weight as more relevant in the Th17 literature (the list of genes is in Sup. file output_with_kuchroo.txt). The data is represented in a network diagram (Extended Data Figure 6) where a co-co-occurrence analysis highlighted genes that were commonly identified in across several studies.

The enrichment analysis revealed that positive and negative information elements were not distributed equally thus indicating information values were not distributed by chance in any of the three time steps, and that these changed over time according to the theoretical and biological expectations. That is, at early stages the naïve cell has two strong set of genes that act as handles to steer the network towards or away from randomness with a larger component of negative elements that indicate signals that are either activating the cells or perturbing cells of the stable naïve cells that are key to the original (undifferentiated steady state) program, then cells are activated and less number of negative genes are present while there is a distribution skew of the positive patch towards neutral elements that pinpoint the evolving genes from the cell activation for differentiation (high peak in the enrichment analysis), at the final step the cells do not longer have negative elements indicating the program has reached some steady state and the cells have mostly been fully differentiated with all remaining elements either positive or closer to information neutral.

CellNet Waddington landscape

CellNet is a network biology-based computational platform that more assesses the fidelity of cellular engineering and claims to generate hypotheses for improving cell derivations[45]. We merged networks of same tissue type into a single larger. The result led to a set of network of networks of the following 16 Homo Sapiens cell types: B-cell, colon, endothelial, esc (embryonic stem cell), fibroblast, heart, hspc (Hematopoietic stem cells), kidney, liver, lung, macrophage, muscleSkel, neuron, ovary, skin and tcell each of the following vertex count: 12006, 4779, 5098, 16581, 8124, 6584, 21758, 5189, 4743, 1694, 5667, 6616, 10665, 1623, 3687 and 11914 on which we applied the causal calculus and reprogrammability measures (Supplement Section 1).
A Waddington landscape can be derived from the location in the complexity and programmability quadrants according to the theoretical expectation. According to Fig. 4e, more differentiated cells tend to be closer to x = 0 while non-differentiated ones tend to be farther

away because they start from a state of randomness with shallow attractors and are very sensitive to perturbations but they can only move in one direction towards creating functions represented by structures moving away from randomness. And this is exactly what we found when calculating and plotting the CellNet networks from 16 cell lines in Homo Sapiens. The cells from the CellNet networks were organized in about the same shape as in the theoretical sketch (Extended Data Figure 3) describing the thermodynamic-like behaviour and in agreement with the biological stage expectation placing stem cells in order (hspc and esc) closer to randomness and high in reprogrammability conforming with the theoretical expectation to have the greatest number of possible shallow attractors with the network only possible move away from randomness followed by blood-related cells (bcell and tcell) that are known to be highly programmable and adaptable followed by the bulk of differentiated cells on first and second quadrants. The distribution of (re)programmability of cells as represented by networks from CellNet fit the natural expected (re)programmability (c.f. Supplement Section 1 and Fig. 4e).

SI SECTION 2 REFERENCES

1. Zenil, Hector; Kiani, Narsis;Tegner, J. Low-algorithmic-complexity entropy-deceiving graphs. *Phys. Rev. E - Stat. Nonlinear, Soft Matter Phys.* (2017).
2. Li, M. & Vitanyi, P. M. B. *An Introduction to Kolmogorov Complexity and Its Applications*. (Springer International Publishing, 2008).
3. Kolmogorov, A. N. Three approaches to the quantitative definition of information. *Probl. Peredachi Informatisii* **1,** 3–11 (1965).
4. Chaitin, G. J. ON THE LENGTH OF PROGRAMS FOR COMPUTING FINITE BINARY SEQUENCES. *ACM* **13,** 547–569 (1966).
5. Calude, C. S. & Stay, M. A. Most programs stop quickly or never halt. **40,** 295–308 (2008).
6. Gac, P. On the symmetry of algorithmic information. **15,** 1477–1480 (1974).
7. Schnorr., C.-P. *Zufälligkeit und Wahrscheinlichkeit. Eine algorithmische Begründung der Wahrscheinlichkeitstheorie.* (1971).
8. Martin-Löf, P. The Definition of Random Sequences. *Inf. Control* **9,** 602–619 (1966).
9. Solomonoff, R. J. A Formal Theory of Inductive Inference. Part I. *Inf. Control* **7,** 1–22 (1964).
10. Hirschfeldt., R. D. and D. R. *Algorithmic Randomness and Complexity*. (Springer Berlin Heidelberg, 2010).
11. Nies, A. *Computability and randomness*. (oxford univeristy press, 2009).
12. Chaitin, G. J. ALGORITHMIC INFORMATION THEORY. **21,** 350–359 (1977).
13. Levin, L. A. Laws of information conservation (nongrowth) and aspects of the foundation of probability theory. 206–210 (1974).
14. Kirchherr, W., Li, M. & Vitányi, P. The Miraculous Universal Distribution. *Math. Intell.* **19,** (1997).
15. Delahaye, J. & Zenil, H. Numerical evaluation of algorithmic complexity for short strings : A glance into the innermost structure of randomness. *Appl. Math. Comput.* **219,** 63–77 (2012).
16. Soler-Toscano, F., Zenil, H., Delahaye, J.-P. & Gauvrit, N. Calculating Kolmogorov complexity from the output frequency distributions of small Turing machines. *PLoS One* **9,** e96223 (2014).
17. Zenil, H. in *Computability of the World? Philosophy and Science in the Age of Big Data* (eds. Ott, M., Pietsch, W. & Wernecke, J.) (Springer International Publishing, 2016).

18. Rado, T. On Non-Computable Functions. *Bell Syst. Tech. J.* 877–884 (1962).
19. Lin, S. & Rado, T. Computer Studies of Turing Mlachine Problems. *J. Assoc. Comput. Mach.* **12,** 196–212 (1965).
20. Brady, A. H. The Determination of the Value of Rado ' s Noncomputable Function $| sum (k) $ for Four- State Turing Machines. *Math. Comput.* **40,** 647–665 (1983).
21. Joosten, J. J., Soler-Toscano, F. & Zenil, H. Fractal dimension versus computational complexity. **2016,** 1–30 (2013).
22. Zenil, H., Soler-Toscano, F., Kiani, N. A., Hernández-Orozco, S. & Rueda-Toicen, A. A Decomposition Method for Global Evaluation of Shannon Entropy and Local Estimations of Algorithmic Complexity. 1–48 (2016). at <http://arxiv.org/abs/1609.00110>
23. Zenil, H., Soler-toscano, F. & Dingle, K. Correlation of automorphism group size and topological properties with program-size complexity evaluations of graphs and complex networks. *Physica A* **404,** 341–358 (2014).
24. Brendan D McKay. Practical graph isomorphism. *Congr. Numer.* **30,** 45–87 (1981).
25. Mckay, B. D. & Piperno, A. Practical graph isomorphism, II. *J. Symb. Comput.* **60,** 94–112 (2014).
26. Albert, R., Jeong, H. & Barabasi, A. L. Error and attack tolerance of complex networks. *Nature* **406,** 378–382 (2000).
27. Shen-orr, S. S., Milo, R., Mangan, S. & Alon, U. Network motifs in the transcriptional regulation network of Escherichia coli. **31,** (2002).
28. Buhrman, H., Li, M., Tromp, J. & Vitányi, P. Kolmogrov Random Graphs and the Incompressibility Method. *Soc. Ind. Appl. Math.* **29,** 590–599 (1999).
29. Antunes, L., Matos, A., Souto, A. & Vitányi, P. Depth as Randomness Deficiency. 724–739 (2009). doi:10.1007/s00224-009-9171-0
30. Hopfield, J. J. Neural networks and physical systems with emergent collective computational abilities Biophysics : Hopfield I T ., V . **79,** 2554–2558 (1982).
31. Hinton, G. E. & Sejnowski, T. J. Optimal perceptural inference. *Proc. IEEE Conf. Comput. Vis. Pattern Recognit.* 0–5 (1983).
32. Kauffman, S. a. Metabolic stability and epigenesis in randomly constructed genetic nets. *J. Theor. Biol.* **22,** 437–467 (1969).
33. Aldana, M. Boolean dynamics of networks with scale-free topology. *Phys. D Nonlinear Phenom.* **185,** 45–66 (2003).
34 Zenil, H, Kiani N.A. and Tegnér J. Methods of Information Theory and Algorithmic Complexity for Network Biology. *Seminars in Cell and Developmental Biology*, vol. **51**, pp. 32-43, 2016.
35. Yosef, N. *et al.* Dynamic regulatory network controlling TH17 cell differentiation. *Nature* **496,** 461–8 (2013).
35. Lee, Y. & Kuchroo, V. Defining the functional states of Th17 cells. *F1000Research* **4,** 1–7 (2015).
36. Lee, Y. *et al.* Induction and molecular signature of pathogenic TH17 cells. *Nat. Immunol.* **13,** 991–9 (2012).
37. Hong, T., Xing, J., Li, L. & Tyson, J. J. A mathematical model for the reciprocal differentiation of T helper 17 cells and induced regulatory T cells. *PLoS Comput. Biol.* **7,** e1002122 (2011).
38. Tuomela, S. *et al.* Identification of early gene expression changes during human Th17 cell differentiation. *Blood* **119,** e151-60 (2012).
39. Ciofani, M. *et al.* A validated regulatory network for Th17 cell specification. *Cell* **151,** 289–303 (2012).

40. Ghoreschi, K. *et al.* Generation of pathogenic T(H)17 cells in the absence of TGF-β signalling. *Nature* **467,** 967–71 (2010).
41. Carneiro, J., Chaouiya, C. & Thieffry, D. Diversity and Plasticity of Th Cell Types Predicted from Regulatory Network Modelling. **6,** 9–12 (2010).
42. Gaublomme, J. T. *et al.* Single-Cell Genomics Unveils Critical Regulators of Th17 Cell Pathogenicity. *Cell* 1–13 (2015). doi:10.1016/j.cell.2015.11.009
43. Zhu, J., Yamane, H. & Paul, W. E. Differentiation of Effector CD4 T Cell Populations [*]. *Annu. Rev. Immunol.* **28,** 445–489 (2010).
44. Cahan, P. *et al.* CellNet: Network Biology Applied to Stem Cell Engineering. *Cell* **158,** 903–915 (2014).

Extended Data Figures

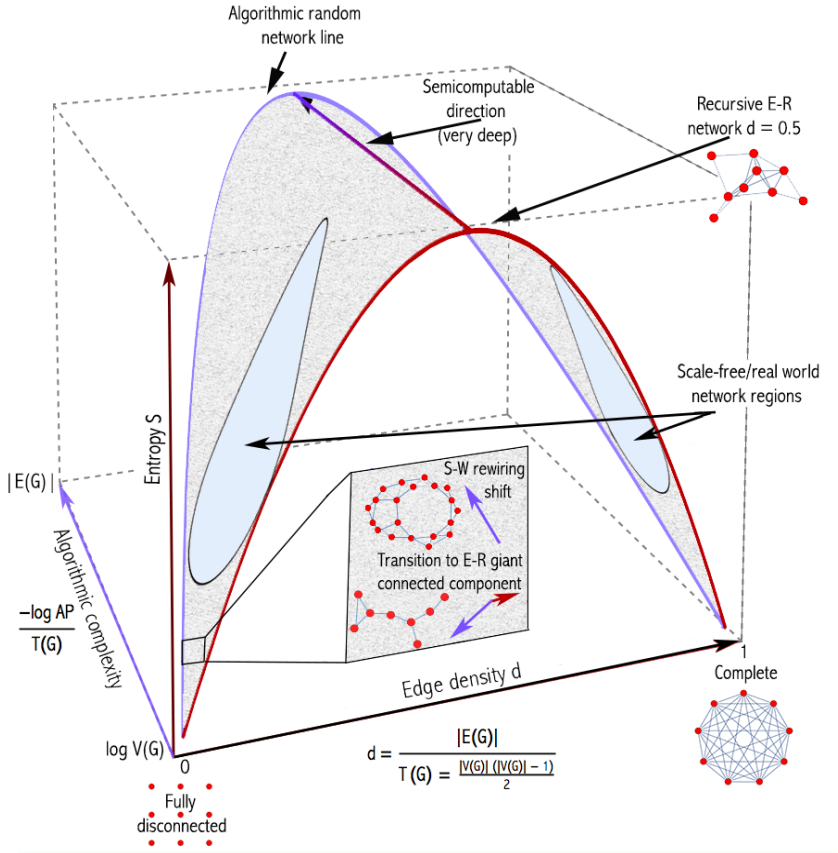

Extended Figure 1: Algorithmic complexity (numerically approached by way of Algorithmic Probability) adds an additional dimension (depth), complementary but different from to the notion of entropy, when performing network analysis. Unlike statistical mechanical approaches such as Shannon Entropy (for strings or networks), algorithmic complexity improves over Entropy by assigning lower Entropy and thus higher causal content to objects that do not only appear statistically simple but also algorithmically simple by having a short generating mechanism capable of reproducing the causal content of a network. Without such additional dimension, causal and no-causal networks are collapsed into the same typical Bernoulli distribution. Indeed, a random-looking network with maximal Shannon entropy can be recursively be generated by a short algorithm that Entropy would misclassify as random. This additional dimension that we introduce in the study of dynamic systems, in particular networks, together with methods and tools, is thus key to better tackle the problem of revealing first principles and discover causal mechanisms in dynamic evolving systems. The new dimension can account for all type of structures and properties and is sensitive in both directions where computable or statistical measures would not. Indeed, for example, an Erdös-Rényi graph can be either recursive or not, recursive means that it is actually pseudo-random and only has the properties of a random graph but is not algorithmic random. This distinction is key in science, where evolving systems may be random-looking but are governed by rules that are otherwise concealed by apparent noise.

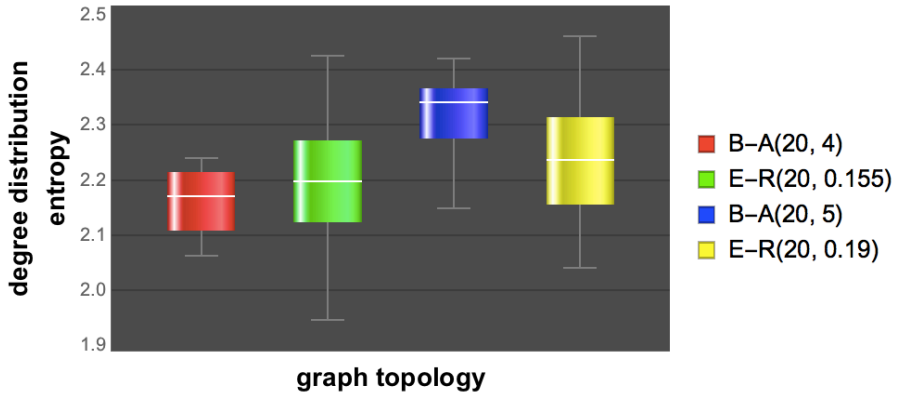

Extended Figure 2: Entropy can easily be fooled; here is a preferential attachment algorithm (B-A) creating networks of growing density (edge number per node) showing how Entropy when calculated on adjacency matrices by only capturing graph density by assigning dense B-A graphs higher entropy than Erdös-Rényi (E-R) graphs. This result was reproduced in 30 replicates using 20 node graphs 20 replicates/graph and experiment was repeated approximately 10 times[1]. Main Fig2c shows another graph created recursively (and thus of low algorithmic complexity) that suggests divergent values of Entropy for the same object but with different descriptions suggesting different probability distributions. A different more robust approach to characterize networks and systems is thus needed to be able to tell these cases apart and improve over traditional techniques that are heavily based upon statistical mechanics by moving into the algorithmic mechanics/calculus here introduced.

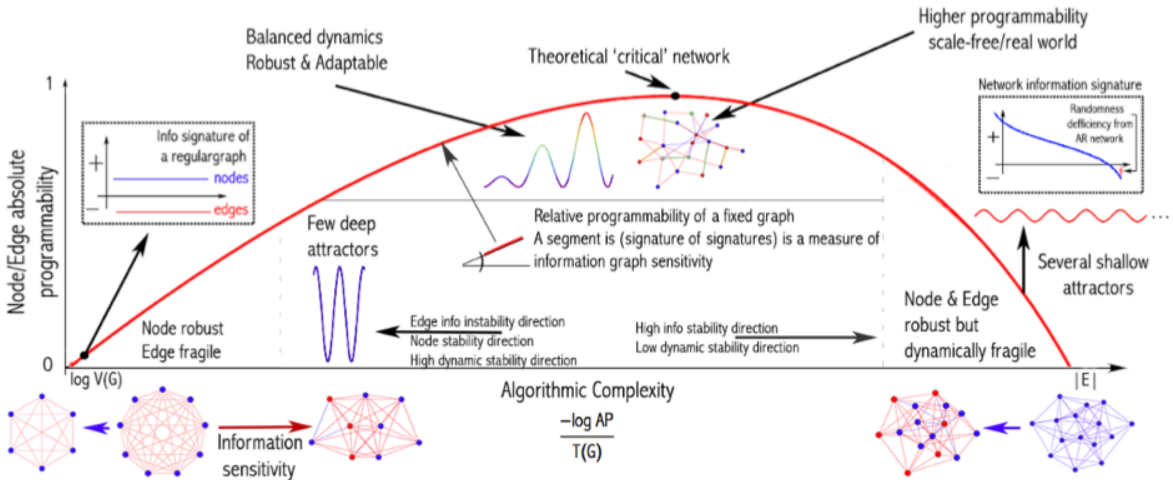

Extended Figure 3. A thermodynamic-like effect based on (re)programmability, a measure of sophistication: Moving random networks by edge removal is significantly more difficult than moving simple networks towards randomness. For random graphs, there are only a few elements, if any, that can be used to move it slowly towards simplicity. In contrast, a greater number of elements can move a simple network faster towards randomness. This relationship, described by the reprogrammability rate $\Delta(G) < \Delta(G')$ (see Sup Mat) for G simple and G' random

graphs of the same size (vertex count), induces a thermodynamic-like asymmetry based on algorithmic probability and reprogrammability. A MAR graph, which is of highest algorithmic randomness, has Δ(MAR) = log n for all its elements after n element removals and thus cannot be easily moved towards greater randomness. This reprogrammability landscape is thus also expected to be related to the dynamical space (epigenetic) landscape with controlled effects in the phase space according to the complexity and the reprogrammability indexes of a system because simple connected graphs have fewer attractors than random graphs of the same size. As we have found and reported in the main text and S.I., moving connected networks towards randomness tends to increase the number of attractors (and therefore make them shallower) providing key insights into the epigenetic Waddington landscape and a tool to move systems and networks hitherto impossible to perform in optimal ways other than by actual simulation. Conversely, moving connected networks away from randomness will tend to reduce the number of attractors (and thereby increase the depth of the remaining ones).

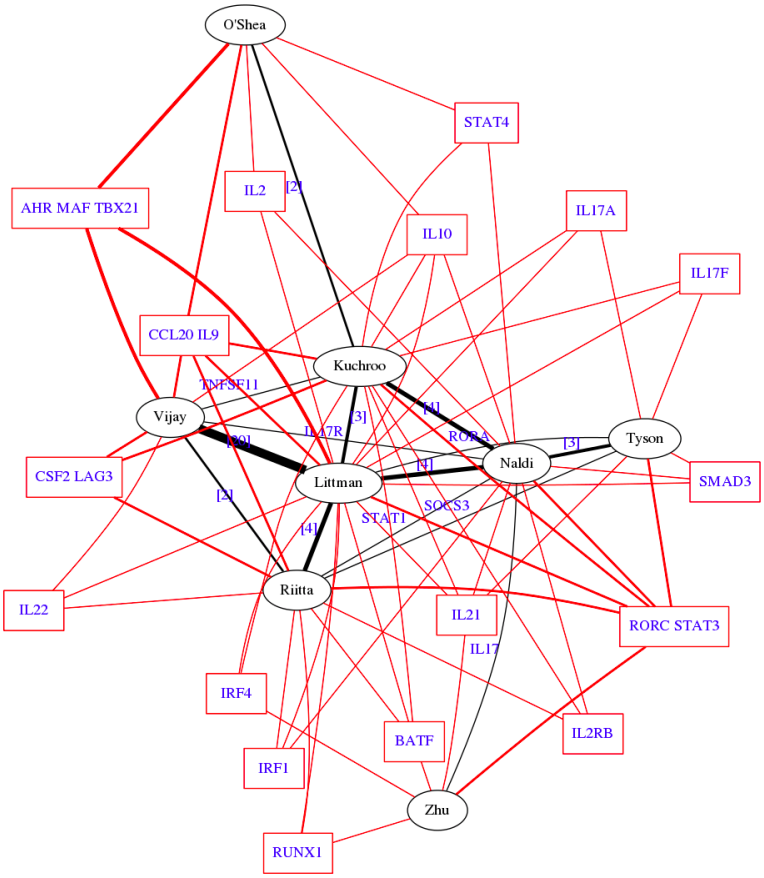

Extended Figure 4: Network Venn diagram of genes (square nodes) occurring in the 9 major papers in the literature (black elliptic nodes) covering investigations of Th17 cells [2–10]. These papers cover the majority genes which have been associated to Th17 cells. Linked genes in the figure are genes found in common between two or more papers. Black lines show the number of genes found in common between two papers (with the thickness denoting the size of the

overlap). These genes were used in main Figure 4f,g,h in the gene enrichment analysis of the Th17 differentiation network.

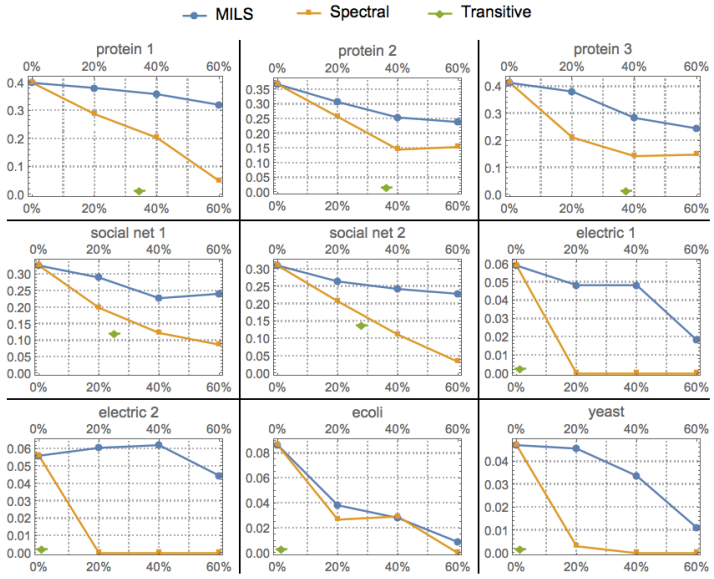

Extended Figure 5: Evaluating MILS using 9 benchmark networks common in the literature [11] in the ability of MILS to preserve the clustering coefficient of the original networks while removing up to 60% of all the network edges against two state-of-the-art network dimensionality reduction methods [12]. Similarly, MILS preserved edge betweeness, degree distribution (see Main Figure 1 l-p) and information signatures (by design) better than other methods such as random edge/node deletion and lowest degree node deletion. This is expected because all these properties of a network are part of its description, MILS thus minimizes the loss of information by maximizing the preservation of all the properties of the original networks.

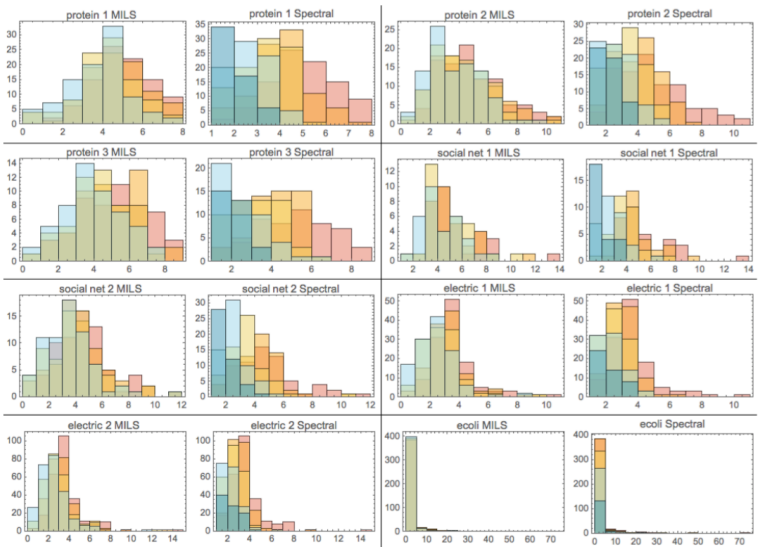

Extended Figure 6. Histograms showing the preservation of degree distributions by MILS against a benchmark dimensionality-reduction algorithm based on graph spectra that maximizes the preservation of the graph eigenvalues when removing 20% of the edges (blue), 40% (yellow), 60% (orange) and 80% (pink). The green colour represents the overlapping of areas for each graph and each method. The graphs used are a set of benchmarking graphs in the literature[11].

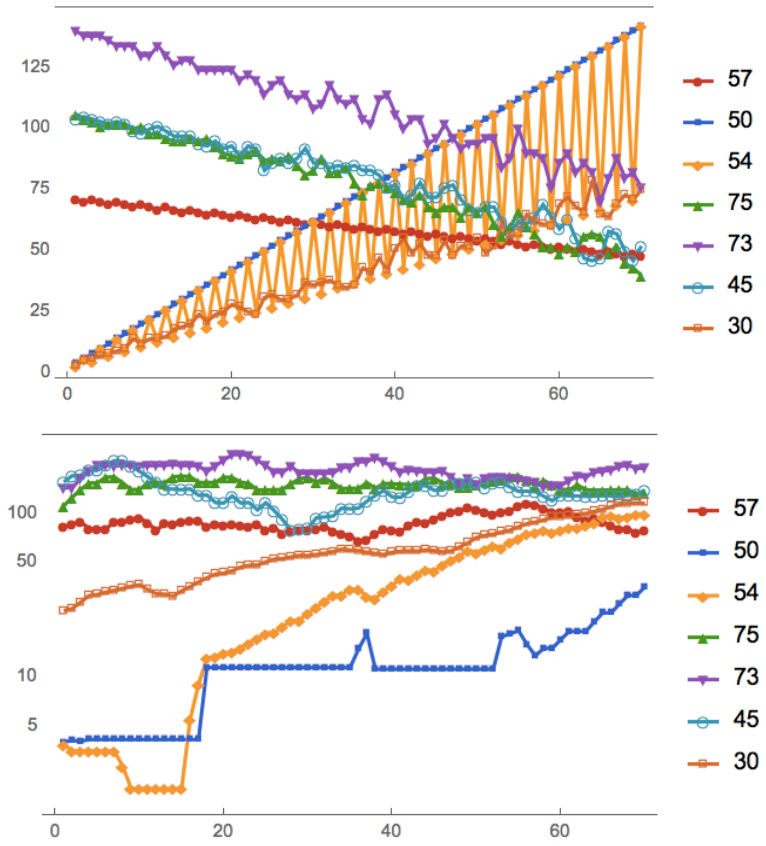

Extended Figure 7. Qualitative reconstruction by representing each row in a CA as a binary vector, which produce a 2n+1 dimensional phase space, where n is the CA runtime for a sample of representative ECAs. The hamming distance between the binary vectors, is used to calculate the behaviour of the moving particle indicating the state of the ECA (top plot). Applying the same procedure to the hypothesized generating mechanism, as identified from our causal calculus, we find that the moving average (bottom plot) of the predicted particle qualitatively moves in a similar fashion (e.g. increasing v decreasing/constant) than the original ECA, and the order among the lines correspond to the original one.

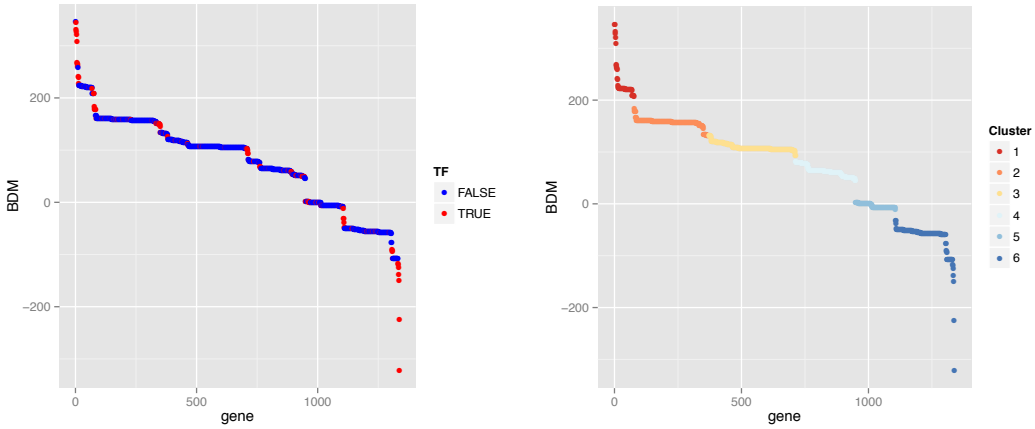

Extended Figure 8. Six clusters were selected using partitioning around medoids clustering. The number of clusters was estimated by optimum average silhouette width.

	GO.ID	Term	Pval
Cluster 1	GO:0006094	gluconeogenesis	1.60E-06
	GO:0006096	glycolysis	0.00036
	GO:0008615	pyridoxine biosynthetic process	0.0124
	GO:0009255	Entner-Doudoroff pathway	0.0124
	GO:0042330	taxis	0.02035
	GO:0016052	carbohydrate catabolic process	0.02911
2	-	-	-
3	-	-	-
4	-	-	-
5	-	-	-
III	GO:0006793	phosphorus metabolic process	2.10E-08
	GO:0009252	peptidoglycan biosynthetic process	2.90E-07
	GO:0006777	Mo-molybdopterin cofactor biosynthetic process	1.20E-05
	GO:0009086	methionine biosynthetic process	0.0027
	GO:0009242	colanic acid biosynthetic process	0.0124
	GO:0006164	purine nucleotide biosynthetic process	0.0196
	GO:0009228	thiamine biosynthetic process	0.0254
	GO:0009243	O antigen biosynthetic process	0.0254

Extended Figure 9. Gene Ontology **GO** database (Biological Process category): over-represented categories tested with TopGO weight01 method (Fisher p<0.05)

	KEGG ID	Term	Pval
Cluster 1	00010	Glycolysis / Gluconeogenesis	1.76E-08
	00051	Fructose and mannose metabolism	7.13E-06
	02030	Bacterial chemotaxis	6.32E-05
	02020	Two-component system	7.55E-04
	00620	Pyruvate metabolism	4.08E-03
	00030	Pentose phosphate pathway	5.14E-03
	02060	Phosphotransferase system (PTS)	5.45E-03
	00680	Methane metabolism	6.70E-03
	01110	Biosynthesis of secondary metabolites	9.59E-03
	01120	Microbial metabolism in diverse environments	1.44E-02
2	-	-	-
3			
4	-	-	-
5	-	-	-
6	00550	Peptidoglycan biosynthesis	1.01E-07
	01100	Metabolic pathways	6.74E-04
	04122	Sulfur relay system	4.11E-03
	00621	Dioxin degradation	9.20E-03
	00622	Xylene degradation	9.20E-03
	00360	Phenylalanine metabolism	1.48E-02
	00300	Lysine biosynthesis	2.48E-02
	00230	Purine metabolism	3.50E-02
	00670	One carbon pool by folate	3.73E-02

Extended Figure 10. Over-represented **KEGG** pathways database (p<0.05)

	EcoCyc pathway	Term
Cluster 1	superpathway of glycolysis and Entner-Doudoroff	5.37E-07
	Sugar Alcohols Degradation	4.82E-06
	superpathway of hexitol degradation (bacteria)	1.91E-05
	glycolysis I (from glucose-6P)	1.91E-05
	glycolysis II (from fructose-6P)	1.91E-05
	gluconeogenesis I	2.56E-04
	Gluconeogenesis	2.56E-04
	Sugar Derivatives Degradation	0.003115401
	Secondary Metabolites Degradation	0.003131693

	superpathway of glycolysis, pyruvate dehydrogenase, TCA, and glyoxylate bypass	0.004830985
	TCA cycle	0.004830985
	Glycolysis	0.005196795
	Generation of Precursor Metabolites and Energy	0.005701038
	sedoheptulose bisphosphate bypass	0.037381258
	Entner-Duodoroff Pathways	0.037381258
	Entner-Doudoroff pathway I	0.037381258
	CpxAR Two-Component Signal Transduction System	0.037381258
	Signal transduction pathways	0.045972995
2	-	-
3	-	-
4	-	-
5	-	-
Cluster 6	methylphosphonate degradation I	9.40E-06
	Phosphorus Compounds Metabolism	9.40E-06
	Methylphosphonate Degradation	9.40E-06
	Pyrimidine Nucleobases Degradation	0.003167986
	Uracil Degradation	0.003167986
	uracil degradation III	0.003167986
	peptidoglycan biosynthesis (meso-diaminopimelate containing)	0.003167986
	Peptidoglycan Biosynthesis	0.003167986
	Cell Wall Biosynthesis	0.003167986
	putrescine degradation II	0.005063846
	3-phenylpropionate and 3-(3-hydroxyphenyl)propionate degradation	0.018877832
	proline to cytochrome bo oxidase electron transfer	0.019695489
	UDP-N-acetylmuramoyl-pentapeptide biosynthesis I (meso-DAP-containing)	0.028546946
	UDP-N-Acetylmuramoyl-Pentapeptide Biosynthesis	0.028546946
	2-oxopentenoate degradation	0.04015748
	Putrescine Degradation	0.0413727
	Pyrimidine Nucleotides Degradation	0.06959294
	superpathway of ornithine degradation	0.075477235
	Purine Nucleotides De Novo Biosynthesis	0.075477235
	superpathway of purine nucleotides de novo biosynthesis II	0.075477235
	superpathway of arginine, putrescine, and 4-aminobutyrate degradation	0.09681385
	L-rhamnose degradation I	0.09815362
	L-rhamnose Degradation	0.09815362

Extended Figure 11. Over-represented **EcoCyc pathways** (FDR<0.05)

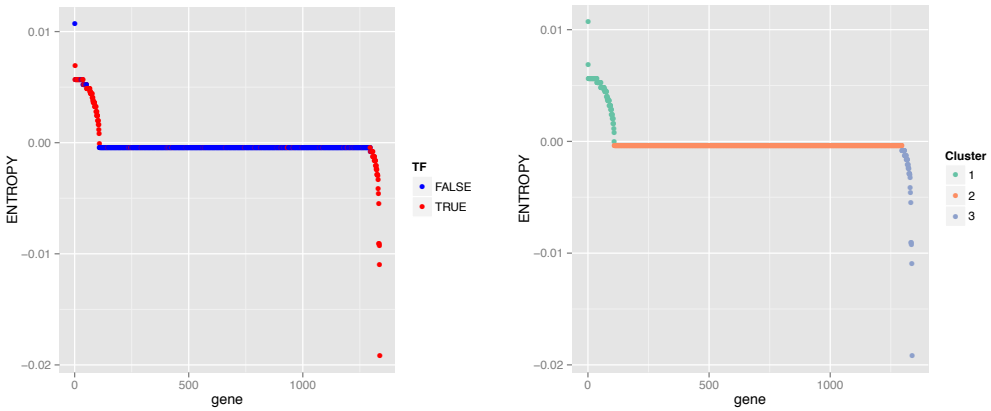

Extended Figure 12. Three clusters (above baseline, baseline, below baseline) were identified for Entropy which proved to be less sensitive, clustering most elements over the X axis. Non-baseline nodes are enriched for Transcription Factors.

	GO.ID	Term	Pval
Cluster 1	GO:0006805	xenobiotic metabolic process	0.0033
	GO:0009268	response to pH	0.0147
	GO:0006355	**regulation of transcription**, DNA-dependent	0.0298
Cluster 2	GO:0006457	protein folding	0.025
Cluster 3	GO:0009255	Entner-Doudoroff pathway	0.0023
	GO:0009435	NAD biosynthetic process	0.0108

Extended Figure 13. Gene Ontology (Biological Process): over-represented categories tested with TopGO weight01 method (Fisher p<0.05) using Shannon Entropy. No significant groups after GO enrichment analysis were found.

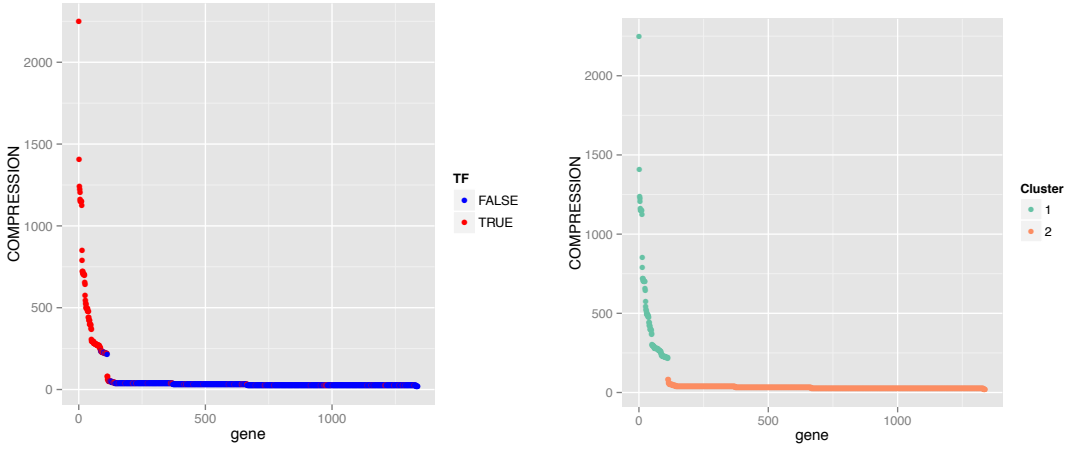

Extended Figure 14. Two clusters identified using Compress (above baseline, baseline). Above-baseline nodes are enriched for Transcription Factors. No significant groups after GO enrichment analysis were found.

	GO.ID	Term	Pval
Cluster 1	GO:0006805	xenobiotic metabolic process	0.003
	GO:0009255	Entner-Doudoroff pathway	0.014
	GO:0006355	**regulation of transcription**, DNA-dependent	0.029
Cluster 2	-	-	

Extended Figure 15. Gene Ontology (**Biological Process**): Over-represented categories tested with TopGO weight01 method (Fisher p<0.05) using lossless compression (Compress algorithm).

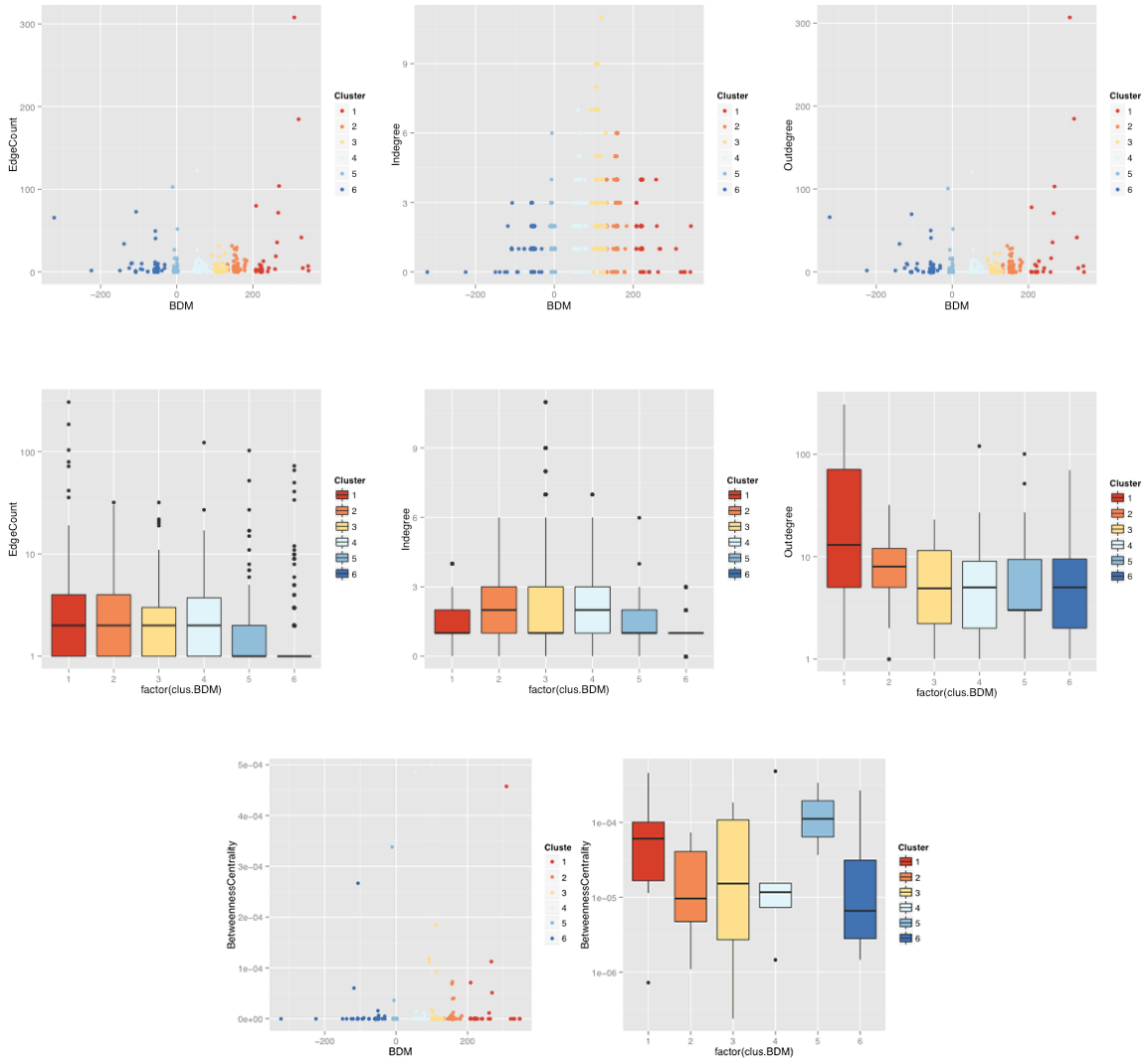

Extended Figure 16. Unlike graph-theoretic measures that can be described as single or composed function of other graph-theoretic measures, BDM was not found to correlate with any of these measures, just as it did not correlate with lossless compression and Shannon entropy. Control Experiments: All attempts to produce statistical significant clusters from graph-theoretic measures, lossless compression and Shannon entropy failed when tested against the same Gene Ontology databases.

EXTENDED FIGURES REFERENCES

1. Zenil, Hector; Kiani, Narsis;Tegner, J. Low-algorithmic-complexity entropy-deceiving graphs. *Phys. Rev. E - Stat. Nonlinear, Soft Matter Phys.* (2017).
2. Yosef, N. *et al.* Dynamic regulatory network controlling TH17 cell differentiation. *Nature* **496,** 461–8 (2013).
3. Lee, Y. *et al.* Induction and molecular signature of pathogenic TH17 cells. *Nat. Immunol.* **13,** 991–9 (2012).
4. Hong, T., Xing, J., Li, L. & Tyson, J. J. A mathematical model for the reciprocal differentiation of T helper 17 cells and induced regulatory T cells. *PLoS Comput. Biol.* **7,** e1002122 (2011).
5. Tuomela, S. *et al.* Identification of early gene expression changes during human Th17 cell differentiation. *Blood* **119,** e151-60 (2012).
6. Ciofani, M. *et al.* A validated regulatory network for Th17 cell specification. *Cell* **151,** 289–303 (2012).
7. Ghoreschi, K. *et al.* Generation of pathogenic T(H)17 cells in the absence of TGF-β signalling. *Nature* **467,** 967–71 (2010).
8. Carneiro, J., Chaouiya, C. & Thieffry, D. Diversity and Plasticity of Th Cell Types Predicted from Regulatory Network Modelling. **6,** 9–12 (2010).
9. Gaublomme, J. T. *et al.* Single-Cell Genomics Unveils Critical Regulators of Th17 Cell Pathogenicity. *Cell* 1–13 (2015). doi:10.1016/j.cell.2015.11.009
10. Zhu, J., Yamane, H. & Paul, W. E. Differentiation of Effector CD4 T Cell Populations *. *Annu. Rev. Immunol.* **28,** 445–489 (2010).
11. Milo, R. Shen-Orr, S. Itzkovitz, N. Kashtan, D. Chklovskii, U. A. Network Motifs: Simple Building Blocks of Complex Networks. *Science (80-.).* **298,** 824–827 (2002).
12. Zenil, H., Kiani, N. & Tegnér, J. Quantifying Loss of Information in Network-based Dimensionality Reduction Techniques. *J. complex networks* 1–30 (2015). at <http://arxiv.org/abs/1504.06249>
13. Soler-Toscano, F., Zenil, H., Delahaye, J.-P. & Gauvrit, N. Calculating Kolmogorov complexity from the output frequency distributions of small Turing machines. *PLoS One* **9,** e96223 (2014).